

## إقرار

أنا الموقع أدناه مقدم الرسالة التي تحمل العنوان:

# **Dye-Sensitized Solar Cell Using Natural Dyes Extracted From Dried Flowers**

أقر بأن ما اشتملت عليه هذه الرسالة إنما هي نتاج جهدي الخاص، باستثناء ما تمت الإشارة إليه حيثما ورد، وأن هذه الرسالة ككل، أو أي جزء منها لم يقدم من قبل لنيل درجة أو لقب علمي أو بحث لدى أية مؤسسة تعليمية أو بحثية أخرى.

## **DECLARATION**

The work provided in this thesis, unless otherwise referenced, is the researcher's own work, and has not been submitted elsewhere for any other degree or qualification.

Student's name: **Hussein A. Al Mogiar**

اسم الطالب: **حسين أمين المغير**

Signature:.....

التوقيع:

Date: 09/09/2015

التاريخ:

**Islamic University of Gaza  
Deanery of Higher Studies  
Faculty of Science  
Department of Physics**



## **Dye-Sensitized Solar Cell Using Natural Dyes Extracted From Dried Flowers**

الخلايا الشمسية ذات الأصباغ الطبيعية المستخلصة من الزهور المجففة

**By**

**Hussein Amin Al Mogiar**

**B.Sc. in Physics, Islamic University of Gaza**

**Supervisors**

**Dr. Sofyan A. Taya**

**Associate Professor of Physics**

**Dr. Taher M. El-Agez**

**Associate Professor of Physics**

**Submitted to the Faculty of Science as a Partial Fulfillment of the Master Degree  
of Science (M. Sc.) in Physics**

**1436 – 2015**



## **Dedication**

This thesis is dedicated to:

My great teacher Prophet Muhammad

(May Allah bless and grant him)

who taught us the purpose of life,

My homeland Palestine; the warmest womb,

The great martyrs and prisoners; the symbol of sacrifice,

My heart mother; for here endless love, support and encouragement,

My dear father; who never stop giving of themselves in countless ways,

My beloved brothers; Abed Allah and Ahmed whom my support in life,

My dearest wife; who stands by me when things look bleak

and the symbol of love and support,

My beloved kids: Rim, Raghad, Fatmeh and Anas; whom I can't force myself

to stop loving,

All friends and family; who encourage and support me all the time,

I dedicate this research

*Hussein Amin Al Mogiar*

## **Acknowledgments**

In the name of Allah the most compassionate all praise be to Allah, the Lord of the worlds; and prayers and peace be upon Mohamed His servant and messenger.

Firstly, I must acknowledge my limitless thanks to Allah; the Ever-Thankful, for His help and bless. I am totally sure that this work would have never become truth, without His guidance.

I owe a deep debt of gratitude to our university for giving us an opportunity to complete this work. I am grateful to my supervisors Dr. Sofyan Taya and Dr. Taher El-Agez for their constant support and whose help, and encouragement helped me in all time of research for arranging and writing of this thesis. I would like to take this opportunity to say warm thanks to Hatem El Ghamri and all my beloved friends; Islam Radwan, Mohammed Dawood and Mohammed Al Qrenawy, Ahmed Al Ghouti, who have been so supportive along the way of doing my thesis. I also would like to express my wholehearted thanks to my father and mother for giving me the love and support. I would like to thank my family for their generous support they provided me throughout my entire life and particularly through the process of pursuing the master degree. Because of their unconditional love and prayers, I have the chance to complete this thesis. I owe profound gratitude to my wife, whose constant encouragement, limitless giving and great sacrifice, helped me accomplish my degree.

Personally, I'd like to thank all those who have helped with their advice and efforts.

## Abstract

In this thesis, dye sensitized solar cells (DSSCs) were prepared using titanium dioxide ( $\text{TiO}_2$ ) as a semiconducting layer spread on transparent conducting fluorine tin oxide (FTO) coated glass using doctor blade method and based on three natural dyes extracted from Hibiscus Rosa Sinensis, Hibiscus Sabdariffa and Rosa Damascena flowers as sensitizers.

Three processes were conducted to improve the performance of prepared solar cells namely pre and post-treatment of  $\text{TiO}_2$  and FTO layers with three acids, changing the pH of the extract solution, and capping  $\text{TiO}_2$  particles with ZnO layer.

Many measurements were conducted on all DSSCs such as UV-Vis absorption spectra in the range of 400 nm to 800 nm of all dyes, J-V characteristic curves under  $100 \text{ mW/cm}^2$  illumination, and impedance spectroscopy under dark and illumination. Many of the photovoltaic parameters of the cells were presented.

The best performance was obtained for the DSSC sensitized with Hibiscus Sabdariffa dye solution without treatment with  $J_{sc}$  of  $1.18 \text{ mA/cm}^2$ ,  $V_{oc}$  of  $0.46 \text{ V}$ , FF of  $0.51$ , and an efficiency  $\eta$  of  $0.28\%$ . When the treatment processes were applied to DSSC sensitized with Hibiscus Sabdariffa, the efficiency was lowered for all treatments. The treatment of the dye solution of Hibiscus Rosa Sinensis with hydrochloric acid to get pH of  $2.0$  showed an efficiency improvement of  $400\%$ .

## Abstract in Arabic

في هذا البحث، تم تحضير الخلية الشمسية الصبغية بواسطة مادة ثاني أكسيد التيتانيوم كطبقة شبه موصلة حيث تشكلت على زجاج (FTO) باستخدام طريقة الدكتور بلاد واعتمدت على ثلاثة أصباغ طبيعية مستخرجة من الزهور وهي زهرة الفونوغراف وزهرة الكركديه وزهرة الجوري.

تم تطبيق ثلاث دراسات لتحسين أداء الخلايا الشمسية وهي معالجة سطح طبقة FTO وطبقة  $TiO_2$  باستخدام ثلاثة أحماض و تأثير تغيير درجة الحموضة لمحلول الأصباغ المستخلصة وتغطية جزيئات مادة ثاني أكسيد التيتانيوم باستخدام طبقة من أكسيد الزنك.

تم قياس الامتصاص الطيفي للصبغات الثلاث وقياس ودراسة منحنيات التيار-الجهد لكل الخلايا تحت شدة إضاءة  $100 \text{ mW/cm}^2$  وقياس الممانعة الطيفية تحت تأثير الالام والإضاءة إضافة إلى عرض كل القيم والمتغيرات الخاصة بالخلايا.

تم الحصول على أفضل نتيجة للخلايا الشمسية الصبغية باستخدام محلول صبغة الكركديه وذلك بدون استخدام أي معالجة حيث كانت  $J_{sc}=1.18 \text{ mA/cm}^2$  و  $V_{oc}=0.46\text{v}$  و  $FF=0.51$  و الكفاءة تساوي 0.28%. عند تطبيق الدراسات المحسنة للكفاءة أظهر استخدام محلول صبغة الكركديه انخفاضا ملحوظا في كل الدراسات. إن معالجة محلول صبغة الفونوغراف باستخدام محلول مخفف من حمض الهيدروكلوريك ليصبح الرقم الهيدروجيني يساوي 2.0 أظهرت زيادة في الكفاءة بقيمة تساوي 400%.

# Contents

Dedication.....	ii
Acknowledgments.....	iii
Abstract.....	iv
Abstract in Arabic.....	v
List of Figures.....	ix
List of Tables.....	xii
Symbols.....	xiv

## Chapter One : Introduction

1.1. History of energy sources.....	1
1.1.1. Non-renewable energy sources.....	1
1.1.2. Renewable energy sources.....	1
1.2. Solar irradiation and availability of solar electricity.....	1
1.3. Air mass.....	2
1.4. Types of solar energy conversion.....	3
1.4.1. Thermal solar energy conversion.....	4
1.4.2. Thermoelectric solar energy conversion.....	4
1.4.3. Photoelectric solar energy conversion.....	4
1.4.4. Chemical solar energy conversion.....	4
1.5. Solar electricity.....	5
1.6. Types of solar cells.....	5
1.6.1. Single-crystalline and polycrystalline silicon solar cells.....	5
1.6.2. Thin film solar cells.....	6
1.6.3. Photoelectrochemical solar cells.....	6
1.7. Electricity problem in Gaza.....	7
1.8. State of the art.....	8
1.9. Aim of this work.....	9

## Chapter Two : Dye-Sensitized Solar Cells (DSSCs)

2.1. Introduction.....	10
2.2. Materials of a dye-sensitized solar cell.....	10
2.2.1. Substrates.....	10

2.2.2. Nanoparticle electrodes.....	10
2.2.3. Sensitizer dyes.....	11
2.2.4. Electrolytes.....	12
2.2.5. Counter-electrode catalysts.....	12
2.2.6. Sealing.....	13
2.3. Operating principle.....	13
2.4. Parameters of solar cells.....	15
2.4.1. Short circuit current density $J_{sc}$ .....	15
2.4.2. Open circuit potential $V_{oc}$ .....	15
2.4.3. Optimum voltage $V_m$ .....	16
2.4.4. Optimum current density $J_m$ .....	16
2.4.5. Fill factor.....	16
2.4.6. Efficiency $\eta$ .....	17
2.4.7. The simple electrical model of a solar cell.....	17

### **Chapter Three : Description of Instruments and Techniques Used in DSSC**

#### **Fabrication**

3.1. Materials used in the preparation of DSSCs.....	19
3.2. Experimental.....	19
3.2.1. Extraction the natural dyes.....	19
3.2.1.1. Measuring absorption spectra of natural dyes.....	19
3.2.2. FTO cleaning.....	20
3.2.3. Preparing of $TiO_2$ film.....	20
3.2.4. Sintering of $TiO_2$ and DSSC assembly.....	20
3.3. Techniques used to improve the efficiency.....	21
3.3.1. FTO acidic treatment.....	21
3.3.2. $TiO_2$ Film acidic treatment.....	21
3.3.3. Effect of changing pH of dyes.....	21
3.3.4. Successive ionic layer absorption and reaction method.....	21
3.4. Description of instruments.....	22
3.4.1. Autolab PGSTAT 302N.....	22
3.4.2. Ultraviolet and visible absorption spectroscopy (UV-Vis).....	25
3.4.3. J-V measurement systems of solar cell.....	25

3.4.4. Diffuse reflectance and Kubelka-Munk.....	26
--	----

## **Chapter Four : Results And Discussion**

4.1. Sensitization of DSSCs by three plant flowers.....	29
4.1.1. Absorption spectra of the extracts.....	29
4.1.2. Photovoltaic parameters.....	30
4.2. FTO acidic treatment.....	34
4.2.1. J-V characterizations.....	34
4.3. Acidic treatment of TiO <sub>2</sub> .....	37
4.3.1. J-V characterizations.....	38
4.4. Effect of the pH of dye solutions.....	41
4.4.1. J-V characterizations.....	41
4.5. Effect of SILAR method to improve the efficiency of DSSCs.....	48
4.6. Electrochemical impedance spectroscopy.....	49
4.6.1. Electrochemical impedance spectroscopy of the untreated cell.....	49
4.6.2. Electrochemical impedance spectroscopy of the DSSC sensitized by Hibiscus Rosa Sinensis with post treated TiO <sub>2</sub> layer with Nitric acid.....	51
4.6.3. Electrochemical impedance spectroscopy of the DSSC sensitized by Hibiscus Rosa Sinensis of pH of 5.5.....	53

## **Chapter Five**

Conclusion.....	60
References.....	62

# List Of Figures

## Chapter One

Figure 1.1 Spectral distribution of solar radiation on: a) the surface of the Sun (black body), b) the top of the Earth's atmosphere (AM0), c) the Earth's atmosphere layer (AM1.5).....	3
--	---

## Chapter Two

Figure 2.1 The working principle of dye-sensitized nanostructured solar cell.....	14
Figure 2.2 Schematic energy diagram.....	14
Figure 2.3 Typical J-V curve of a solar cell showing the open circuit voltage $V_{oc}$ , short circuit current $I_{sc}$ , and the maximum power point $P_m$ .....	16
Figure 2.4 Equivalent circuit of a solar cell including series and shunt resistances..	17
Figure 2.5 Effect of (a) reducing parallel resistance and (b) increasing series resistance.....	18

## Chapter Three

Figure 3.1 Doctor blade method to spread the $TiO_2$ paste on the FTO coated glass.	20
Figure 3.2 The Autolab PGSTAT 302N instrument with frequency response analyzer FRA 32 Module.....	23
Figure 3.3 Nyquist Plots.....	23
Figure 3.4 Bode plot showing the phase angle as a function of frequency.....	24
Figure 3.5 Genesys 10S UV-Vis spectrophotometer.....	25
Figure 3.6 System of I-V measurement and solar cell simulator.....	26
Figure 3.7 Specular reflection diagram.....	26
Figure 3.8 Diffuse reflection diagram.....	27
Figure 3.9 Evolution 220 UV-Visible spectrophotometer instrument with ISA-220 Integrating Sphere Accessory.....	28

## Chapter Four

Figure 4.1 The UV-Vis absorption spectrum of the dyes extracted from Hibiscus Rosa Sinensis, Hibiscus Sabdariffa, Rosa Damascena.....	29
Figure 4.2 Current density-voltage characteristics curves for the DSSCs sensitized by Hibiscus Sabdariffa, Hibiscus Rosa Sinensis and Rosa Damascena.....	30

Figure 4.3 Current density-voltage characteristics curves for the DSSCs sensitized by Hibiscus Sabdariffa, Hibiscus Rosa Sinensis and Rosa Damascena.....	31
Figure 4.4 Molecular structure of anthocyanin and the binding between anthocyanin molecule and TiO <sub>2</sub> particles.....	32
Figure 4.5 Hibiscus Rosa Sinensis, Hibiscus Sabdariffa and Rosa Damascena.....	33
Figure 4.6 Absorption spectra of Hibiscus Rosa Sinensis dye on TiO <sub>2</sub> film and the extract of the same flower in ethanol.....	33
Figure 4.7 Current density-voltage characteristics curves of DSSCs with the pre-treatment of FTO layer with acids sensitized by: (1) Hibiscus Rosa Sinensis (2) Hibiscus Sabariffa (3) Rosa Damascena (4) Hibiscus Rosa Sinensis (5) Hibiscus Sabariffa (6) Rosa Damascena. The upper panels were presented in acids for 5 minutes whereas the lower panels for 10 minutes.....	34
Figure 4.8 Current density-voltage characteristics curves for the DSSCs sensitized by (1) Hibiscus Rosa Sinensis (2) Hibiscus Sabdariffa (3) Rosa Damascena with post-treated TiO <sub>2</sub> film by the acids for 5 minutes.....	38
Figure 4.9 Absorption spectra of Hibiscus Rosa Sinensis extract in ethanol solution and anthocyanin adsorbed onto TiO <sub>2</sub> film treated with HNO <sub>3</sub> , HCl and H <sub>3</sub> PO <sub>4</sub> .....	40
Figure 4.10 Current density-voltage characteristics curves for the DSSCs sensitized by (1) Hibiscus Rosa Sinensis (3) Hibiscus Sabdariffa (5) Rosa Damascena using acetic acid to change pH of the dye, sensitized by (2) Hibiscus Rosa Sinensis (4) Hibiscus Sabdariffa (6) Rosa Damascena using hydrochloric acid to change pH of the dye.....	42
Figure 4.11 DSSC efficiency versus the pH of the extract solution of three dyes using acetic acid.....	44
Figure 4.12 Absorption spectra of Hibiscus Rosa Sinensis extract in ethanol solution and anthocyanin adsorbed onto TiO <sub>2</sub> film of pH of 2 and pH of 5.5.....	46
Figure 4.13 DSSC efficiency versus the pH of the extract solution of three dyes using hydrochloric acid.....	47
Figure 4.14 Current density-voltage characteristics curves for the DSSCs sensitized by Hibiscus Rosa Sinensis using SILAR Method.....	48
Figure 4.15 Nyquist plots of the DSSC sensitized by Hibiscus Rosa Sinensis without any treatment at -0.4 V, -0.6 V and -0.8 V in the dark and under an illumination of 100 mW/cm <sup>2</sup> .....	50

Figure 4.16 The equivalent circuit for the DSSC sensitized by Hibiscus Rosa Sinensis without treatments.....	50
Figure 4.17 Nyquist plots of the DSSC sensitized by Hibiscus Rosa Sinensis with post treated TiO <sub>2</sub> layer with Nitric acid at -0.4 V, -0.6 V and -0.8 V in the dark and under an illumination of 100 mW/cm <sup>2</sup> .....	52
Figure 4.18 The equivalent circuit for the DSSC sensitized by Hibiscus Rosa Sinensis with post treated TiO <sub>2</sub> layer with Nitric acid.....	52
Figure 4.19 Nyquist plots of the DSSC sensitized by Hibiscus Rosa Sinensis of pH of 5.5 at -0.4V in the dark and under an illumination of 100 mW/cm <sup>2</sup> .....	54
Figure 4.20 The equivalent circuit for the DSSC sensitized by Hibiscus Rosa Sinensis of pH of 5.5.....	54
Figure 4.21 Nyquist plots of DSSCs sensitized by Hibiscus Rosa Sinensis at -0.4V applied potential under an illumination of 100 mW/cm <sup>2</sup> .....	56
Figure 4.22 Nyquist plots of DSSCs sensitized by Hibiscus Rosa Sinensis at -0.6V applied potential under an illumination of 100 mW/cm <sup>2</sup> .....	56
Figure 4.23 Nyquist plots of DSSCs sensitized by Hibiscus Rosa Sinensis at -0.8V applied potential under an illumination of 100 mW/cm <sup>2</sup> .....	57
Figure 4.24 Bode plots of DSSCs sensitized by Hibiscus Rosa Sinensis for the three studies mentioned before under an illumination of 100 mW/cm <sup>2</sup> at -0.4 V, -0.6 V, and -0.8 V applied voltages.....	57

## List Of Tables

### Chapter Three

Table 3.1 Flowers used in this study to extract the natural dyes.....	19
---	----

### Chapter Four

Table 4.1 Photovoltaic parameters of the DSSCs sensitized by the three natural Dyes.....	31
Table 4.2 Photovoltaic parameters of the DSSCs using the treated FTO with the acids for 5 minutes.....	35
Table 4.3 Photovoltaic parameters of the DSSCs sensitized by natural dyes using pre- treatment the FTO by acids for 10 minutes.....	36
Table 4.4 Photovoltaic parameters of the DSSCs sensitized by natural dyes using post-treatment of TiO <sub>2</sub> film by acids for 5 minutes.....	38
Table 4.5 Photovoltaic parameters of the DSSCs sensitized by the dyes with changing the values pH using acetic acid.....	41
Table 4.6 Photovoltaic parameters of the DSSCs sensitized by the dyes with changing the values pH using hydrochloric acid.....	44
Table 4.7 Photovoltaic parameters of the DSSCs sensitized by Hibiscus Rosa Sinensis dye using SILAR Method with three different molarities of ZnCl <sub>2</sub> solution.....	48
Table 4.8 Electrochemical impedance spectroscopy results from data-fitting of Nyquist plots to the equivalent circuit model in Fig. 4.28 for the DSSC sensitized by Hibiscus Rosa Sinensis without any treatment.....	51
Table 4.9 Electrochemical impedance spectroscopy results from data-fitting of Nyquist plots to the equivalent circuit model in Fig. 4.30 for the DSSC sensitized by Hibiscus Rosa Sinensis and TiO <sub>2</sub> post-treatment with Nitric acid.....	53
Table 4.10 Electrochemical impedance spectroscopy results from data-fitting of Nyquist plots to the equivalent circuit model in Fig. 4.32 for the DSSC sensitized by Hibiscus Rosa Sinensis of pH of 5.5.....	55

Table 4.11 EIS results from data-fitting of Nyquist plots to the equivalent circuit model in Fig. 4.33 for the DSSCs sensitized by Hibiscus Rosa Sinensis at -0.4V applied voltage.....	58
Table 4.12 EIS results from data-fitting of Nyquist plots to the equivalent circuit model in Fig. 4.34 for the DSSCs sensitized by Hibiscus Rosa Sinensis at -0.6V applied voltage.....	58
Table 4.13 EIS results from data-fitting of Nyquist plots to the equivalent circuit model in Fig. 4.35 for the DSSCs sensitized by Hibiscus Rosa Sinensis at -0.8V applied voltage.....	59
Table 4.14 Electron lifetime calculations from Bode plots.....	59

## Symbols

K	Kelvin degree
W	Watt
m <sup>2</sup>	Meter square
k	Kilo
h	Hour
nm	Nano meter
Si	Silicon
μm	Micro meter
CdTe	Cadmium telluride
a-Si	Amorphous silicon
DSSC	Dye-sensitized solar cells
TiO <sub>2</sub>	Titanium dioxide
ZnO	Zinc oxide
J <sub>sc</sub>	Short circuit current density
V <sub>oc</sub>	Open circuit potential
MW	Megawatt
GPP	Gaza Power Plant
mA	Mille ampere
P <sub>max</sub>	Power maximum
mV	Mille volt
V	Volt
pH	Hydrogen number
Zncl <sub>2</sub>	Zinc dichloride
η	Conversion efficiency
FTO	Fluorine-doped tin oxide (SnO <sub>2</sub> :F)
I <sub>max</sub>	Optimum current
V <sub>max</sub>	Optimum voltage
FF	Fill factor
TCO	Transparent conducting oxide
°C	Celsius degree
eV	Electron volt
g/mol	Gram per mole

$\text{cm}^3$	Centimeter cubic
$\Gamma$	Iodine
$\Gamma^3$	Tri-iodide
Pt	Platinum
$P_{(\text{light})}$	Incident light
J-V	Current density-voltage
$R_s$	Series resistance
$R_{\text{sh}}$	Shunt resistance
$S^*$	Excited energy state of the sensitizer
$S^+$	Oxidized state of the sensitizer
S	Original state
$\nu$	Frequency
$\Delta V$	Voltage difference
$Z'$	Real impedance
$Z''$	Imaginary impedance
EIS	Electrochemical impedance spectroscopy
FRA	Frequency response analyzer
DC	Direct current
AC	Alternative current
Z	Impedance
UV-Vis	Ultraviolet-Visible
SILAR	Successive ionic layer absorption and reaction
P-V	Power-Voltage
a.u.	Arbitrary units
HCl	Hydrochloric acid
$\text{H}_3\text{PO}_4$	Phosphoric acid
$\text{HNO}_3$	Nitric acid
$R_{\text{CT}}$	Charge-transfer resistance
C	Capacitance
CPE	Constant phase element
$Q_0$	Constant phase element coefficient
$\omega_{\text{max}}$	Characteristic frequency
$\tau_{\text{electron}}$	Electron lifetime

# **Chapter One**

## **Introduction**

### **1.1. History of energy sources**

Over the last 200 years, people have become more and more dependent on energy that they dig out of the ground. In the 1700's, almost all the energy came from wind, water, firewood, or muscle power. About 1800, much of the energy was taken from coal dug out of the ground. About 1900, human began to drill for oil and natural gas. By 1950 these "fossil fuels" had mainly displaced the older energy sources except for water power. In some parts of the world new fossil fuels are being formed even today. After 1950, we began to use atomic energy from uranium dug from the ground. Energy sources have been classified into nonrenewable and renewable sources.

#### **1.1.1. Non-renewable energy sources**

Fossil fuels such as coal and natural gas are the main sources of energy used by humans. They come from the decayed remains of prehistoric plants and animals buried in the ground millions of years ago. This type of energy is expected to run out through several decades; and the burning of fossil fuels has caused and is causing damage to the environment of Earth such as raise the air temperature around the Earth's surface. Moreover, they have a direct impact on human health and cause many diseases.

#### **1.1.2. Renewable energy sources**

The renewable energy sources such as sunlight, wind, rain, tides, and geothermal heat are clean, environmentally friendly sources of energy that do not lead to pollution. But they have high cost and low efficiency. If used wisely, however, renewable energy supplies can last forever. Sun has always been the most powerful energy source on Earth. Sunlight can be transformed into electricity using solar cells. Solar cells have found applications in many different fields such as calculators, solar lamps and even on spacecraft and satellites.

### **1.2. Solar irradiation and availability of solar electricity**

The energy of the Sun is created by the nuclear fusion reaction of hydrogen and helium which occurs inside the sun at several million degrees. The solar radiation is

emitted from the Sun's photosphere at (5800-6000)°K temperature. Because all elements are ionized to some degree at this temperature, their spectral lines are strongly broadened so that the gaseous surface of the Sun radiates like a black body as shown in Fig. 1.1 [1]. The solar energy that reaches Earth is determined by the radiation of the Sun and the distance between the Earth and the Sun. The solar radiation power just outside the Earth's atmosphere is 1.353 kW/m<sup>2</sup>, a number also called the solar constant [2]. Passing through the Earth's atmosphere, radiation is partly absorbed by the air molecules, in particular oxygen, water vapor, and carbon dioxide; and attenuated by scattering from air molecules, aerosols and dust particles. Note that only 30% of total solar radiation actually hits the Earth surface perpendicular to the Sun's path. The available solar irradiation in a certain place depends on the latitude, the climatic type in a yearly basis, the season, the time of day, and the weather conditions in a specific time. The total yearly solar irradiation on horizontal surface is 1800-2300 kWh/m<sup>2</sup> in the equator, and 2000-2500 kWh/m<sup>2</sup> in the so called "solar belt" i.e. between 20° and 30° latitude [3].

### 1.3. Air mass

Specific solar radiation conditions are defined by the Air Mass (AM) value. AM is the direct optical path length (atmosphere thickness). The spectral distribution and total flux of radiation just outside the Earth's atmosphere, similar to the radiation of a Sun, has been defined as AM0 meaning zero atmosphere as shown in Fig. 1.1. In passing through the atmosphere the radiation becomes attenuated by complex and varying extinction processes mentioned above. At the equator at sea level at noon when the incidence of sunlight is vertical ( $\alpha=90^\circ$ , sun in zenith) and the light travels the shortest distance through the atmosphere and air (air-mass) to the surface, the spectral solar radiance and flux is defined as AM1. However, if the angle of light incidence is smaller than  $90^\circ$ , the light has to travel through more AM than under AM1 conditions. The relative path length through the atmosphere by the shortest geometrical path is given by:

$$AM = \frac{1}{\sin \alpha} = \frac{1}{I_0} \quad (1.1)$$

where  $I_0$  is path length normal to the earth's surface at sea level and  $\alpha$  is the zenith angle. The so-called AM1.5 conditions are achieved when the sun is at an angle of  $41.8^\circ$  above the horizon and results in the spectral distribution shown in Fig. 1.1. This angle of incidence is commonly encountered in western countries and hence AM1.5 is taken as a standard condition for solar cell testing and referencing [1]. AM1.5 represents the overall yearly average solar irradiation. Therefore, it is an important indicator for photovoltaic measurements, where the sun simulators ought to resemble the solar spectrum as close as possible to the reality. The specific value of 1.5 has been selected in the 1970s for standardization purposes, based on an analysis of solar irradiance data in the conterminous United States [4].

#### 1.4. Types of solar energy conversion

Solar energy emitted by the Sun and reaching the Earth's surface is a form of electromagnetic radiation that is available over a wide spectral range (300–2100 nm) where the visible spectrum range from 400 nm to 800 nm. In order to be used, the radiation needs to be converted into an energy form suitable for our needs.

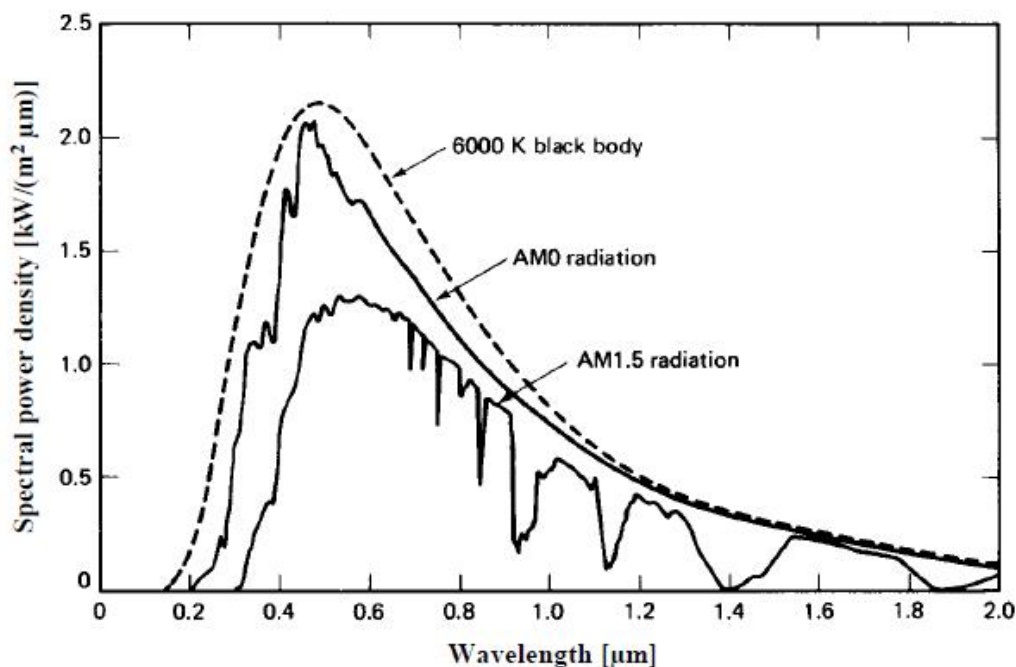


**Fig. 1.1** Spectral distribution of solar radiation on: a) the surface of the Sun (black body), b) the top of the Earth's atmosphere (AM0), c) the Earth's atmosphere layer (AM1.5) [4,5].

The energy of solar radiation is directly utilized in mainly two forms:

- i) direct conversion into electricity that takes place in semiconductor devices called solar cells,
- ii) accumulation of heat in solar collectors [6] .

Four different types of solar energy conversion methods are currently available for this purpose.

#### **1.4.1. Thermal solar energy conversion**

It is a famous type of solar energy conversion. It is used all over the world including Gaza Strip, that observed in the form of black panels on rooftops houses and it is only used to heat water. This type is very effective in summer due to the high density of solar radiation.

#### **1.4.2. Thermoelectric solar energy conversion**

Solar energy is converted into steam which in turn is converted into electricity by rotating turbines in power plants. This technology requires large Sun collection systems and has been applied to construct small to medium sized power plants.

#### **1.4.3. Photoelectric solar energy conversion**

Photovoltaic represents a high-technology approach to converting sunlight directly into electrical energy. The electricity obtained is direct current (dc) and can be used directly to operate direct current devices. The (dc) current supplied by the photovoltaic modules is converted to (ac) power of appropriate frequency using an inverter. The high cost of solar cells is the main factor that limits the wide range use of solar electricity.

#### **1.4.4. Chemical solar energy conversion**

This path represents the conversion of solar energy into chemical energy and is important because of its potential to overcome problems with long term storage and transport of energy. The example of photochemical reactions of this kind is the photocatalytic splitting of water into hydrogen and oxygen.

## **1.5. Solar electricity**

Solar electricity is a growing energy technology today for the huge theoretical potential and the very high practical potential of the solar electricity make it attractive for large-scale utilization. Direct utilization of solar radiation to produce electricity is close to an ideal way to utilize the nature's renewable energy flow. Generating electricity from the sun radiation has many features over other energy generation techniques. The high cost of solar cells has been a significant obstacle for the implementation of the solar electricity in a large scale. There is therefore an urgent need for the development of new materials and concepts for the solar cell technology to reduce this cost [7]. Nanotechnology plays a remarkable role in developing nanoscale materials and utilizing them in the field of solar cells and systems that could potentially lead to realization of low-cost solar cells in the future. These materials include for example different types of synthetic organic materials and inorganic nanoparticles. The solar cells based on these materials are called for example organic solar cells or molecular solar cells.

## **1.6. Types of solar cells**

### **1.6.1. Single-crystalline and polycrystalline silicon solar cells**

The first silicon solar cell was developed by Chapin, Fuller and Pearson at the Bell Telephone Laboratories in the mid 1950's, and it had about 6% efficiency. Today the efficiency of the commercial crystalline silicon solar panels is in the best case about 15% [6,7]. The energy search was accelerated in the late of 20th century. This search resulted in a growing interest in the photovoltaic (PV) solar energy. The major obstacle of using solar cells for terrestrial electricity generation has been a much higher price of the solar electricity when compared to the price of electricity generated from the traditional sources. To produce a solar cell, the semiconductor is doped by the intentional introduction of chemical elements, with which one can obtain a surplus of either positive charge carriers (p-conducting semiconductor layer) or negative charge carriers (n-conducting semiconductor layer) from the semiconductor material. If two differently doped semiconductor layers are combined, then a so-called p-n junction results on the boundary of the layers. At this junction, an interior electric field is built up which leads to the separation of the charge carriers that are released by light. Through metal contacts, an electric charge can be tapped. If

the outer circuit is closed, a consumer is connected, then direct current flows [8]. It is very important to know that over 95% of all the solar cells produced worldwide are composed of the semiconductor material Silicon (Si). As the second most abundant element in earth's crust, silicon has the advantage, of being available in sufficient quantities, and additionally processing the material does not burden the environment. From the manufacturers point of view this is coupled to the need for the special solar cell grade silicon supply and from the market's point of view not very easy to achieve at present PV system costs without governmental subsidies for customers to create artificial markets for the solar electricity.

### **1.6.2. Thin film solar cells**

In order to decrease the material costs of crystalline silicon solar cells, research has been directed to develop low cost thin-film solar cells, which represent the second generation solar cells for terrestrial application. Also as direct band gap semiconductors, the thin film semiconductor materials have much higher absorption coefficient than silicon, and therefore typically less than 1 $\mu$ m thick semiconductor layer is required, which is 100-1000 times less than that of silicon. The amount of expensive semiconductor material is thus reduced, or on the other hand, more expensive semiconductors can be used in the thin films. There are several semiconductor materials that are potential candidates for thin-film solar cells, namely copper indium gallium diselenide, cadmium telluride (CdTe), and hydrogenated amorphous silicon (a-Si). A thin-film solar cell, also called a thin-film photovoltaic cell, is a solar cell that is made by depositing one or more thin layers of photovoltaic material on a substrate. It is expected that the efficiency of commercial second generation solar modules is likely to reach 15%.

### **1.6.3. Photoelectrochemical solar cells**

The oldest type of photovoltaic cell is the photoelectrochemical solar cell, used already by Becquerel for the discovery of the photovoltaic effect in 1839. In the photoelectrochemical solar cell a semiconductor-electrolyte junction is used as a photoactive layer. Michael Grätzel and Brian O'Regan invented "Dye-sensitized solar cells", also called "Grätzel cells", in 1991 [9]. The first cells were only capable of using light at the ultraviolet and blue end of the solar spectrum. By the turn of the century, advances in technology were able to broaden the frequencies in which these

cells were able to respond. The most efficient dyes were simply known as “Black dyes” due to their very dark colors. DSSC is considered the third generation of photovoltaic devices for the conversion of visible light into electric energy. These new types of solar cells are based on the photosensitization produced by the dyes on wide band-gap semiconductors such as  $\text{TiO}_2$  (Titanium dioxide). This sensitization is produced by the dye absorption of part of the visible light spectrum. DSSCs are low cost solar cells because of inexpensive materials and the relative ease of the fabrication processes. Recent studies have shown that metal oxides such as  $\text{TiO}_2$  and  $\text{ZnO}$  (Zinc Oxide) have been successfully used as photo-anode when a dye is adsorbed in the interior of the porous layer of the semiconductor. Even natural dyes extracted from roots, flowers, leaves, fruits, vegetables can be used [10]. The highest efficiency of DSSCs sensitized by Ruthenium complexes adsorbed on nanocrystalline  $\text{TiO}_2$  has reached 12– 15% but they are still not suitable for the high cost and stability.

### **1.7. Electricity problem in Gaza**

Electricity demand in Gaza strip can reach up to 360 megawatts (MW). At its current operating capacity, the Gaza Power Plant (GPP) can produce up to 80 MW; supplemented by 120 MW purchased from Israeli Occupation Authorities and 22 MW from Egypt. The majority of Gazan households have power cuts of at least eight hours per day. Some have no electricity for long as 12 hours a day. For years now, Gaza is suffering from a chronic crisis in the electricity supply. This crisis is an extension of an ongoing series of crises escalating in severity in accordance with the changes in conditions and contexts affecting such crisis. The total amount of electricity available can meet approximately two-thirds of the demand. The chronic electricity deficit affecting Gaza over the past few years has disrupted the delivery of basic services and many fields in the daily life. Since February 2012, the situation has further deteriorated following a sharp decline in the amount of fuel brought into Gaza from Egypt and used to operate the GPP. As a result the people depend on back-up generators. Private mobile generators can be particularly unsafe, environmentally polluting, and are not affordable with the poorest people. The generating capacity and reliability of the GPP has been significantly impaired over the past six years as the destruction of six transformers by an Israeli airstrike in 2006.

Power cuts place immense pressure on Gaza's crumbling electrical grid impacting water and sanitation infrastructure, where lowered hygiene standards. Thus increasing

the pollution level of partially treated sewage discharged into the sea. There is also the risk of back-flow of sewage onto streets, disrupting healthcare delivery and adding misery to the lives of civilians.

### **1.8. State of the art**

In 1991, Grätzel and his co-workers developed a solar cell with energy conversion efficiency exceeding 7%. This solar cell was called the dye sensitized solar cell (DSSC) or the "Grätzel cell" [9]. After its invention, an increasing interest has been shown in the fabrication and development of DSSCs. In 1993, DSSCs gives 10.3% conversion efficiency using a ruthenium dye sensitizer, which contained one ruthenium center and was thus simpler than the ruthenium dye reported in 1991 [10]. In 2001, DSSCs with 10.4% to 11.1% efficiency were fabricated using a ruthenium dye called 'black dye'. Although black dye looks green in solvent, on a porous nanocrystalline-TiO<sub>2</sub> electrode the DSSC looks black, because its wide absorption band covers the entire visible range of wavelengths [11,12]. In 2004, DSSC were assembled using natural dyes extracted from black rice, capsicum, erythrina, variegated flower, Rosa xanthina, and kelp as sensitizers [13]. The  $I_{sc}$  ranging from 0.225 mA/cm<sup>2</sup> to 1.142 mA/cm<sup>2</sup>, the  $V_{oc}$  ranging from 0.412 V to 0.551 V, the fill factor ranging from 0.52 to 0.63, and  $P_m$  ranging from 58 μW to 327 μW were obtained from the DSSC sensitized with natural dye extracts. In 2007, some experimental data for analyzing the various dye's absorption spectra, which can be applied in the DSSC, have been presents [14]. The analysis of dyes focused on the natural dyes which are extracted from the plants and compared with the chemical ones. The results showed that natural dyes have wider absorption spectra than the chemical synthesis due to the more various constituents in the natural dyes. In 2009, The performances of DSSCs assembled by using natural dyes extracted from spinach, amaranth and a mixture of them were investigated [15]. In the sun, the  $V_{oc}$  of cells sensitized by spinach extract was 450 mV, while those sensitized by the mixture showed a  $V_{oc}$  above 500 mV. In 2010, twenty natural dyes, extracted from natural materials such as flowers, leaves, fruits, traditional Chinese medicines, and beverages, were used as sensitizers to fabricate DSSCs. The photoelectrochemical performance of the DSSCs based on these dyes showed that the open circuit voltages ( $V_{oc}$ ) varied from 0.337 to 0.689 V, and the short circuit photocurrent density ( $J_{sc}$ ) ranged from 0.14 to 2.69 mA/cm<sup>2</sup> [15]. Hee-Je Kim, et. all, studied natural dye extracted from Curcuma longa L. The

conversion efficiency was 0.36% that enhanced to 0.6% for the acetic acid-treated curcumin dye [16]. In 2013, The highest efficiency of DSSCs sensitized by Ruthenium complexes adsorbed on nanocrystalline TiO<sub>2</sub> has reached 15% [17]. S. Suhaimi, et. all were assembled the DSSCs using different materials for the semiconductor oxide, dye sensitizer and counter electrode and the conversion efficiency were ranged from 6.7-8.6% [18]. A. Zulkifili, T. Kento, M. Daiki, and A. Fujiki, evaluating the particle size of titania and the effect of the multilayer of TiO<sub>2</sub> [19]. El-Agez et al. studied natural dyes extracted from fresh and dried plant leaves and found that spinach oleracea extract has a better performance after drying where the efficiency of the cell prepared with TiO<sub>2</sub> thin film layer reached 0.29% [20,21]. M. S. Abdel-Latif et al. used Plant seeds as sensitizers and it was found that DSSCs sensitized with the extracts of onion, rapa, and Eruca sativa seeds have efficiencies of 0.875%, 0.86%, and 0.725%, respectively [22]. Kamal S. El-Refi obtained a J<sub>sc</sub> from 0.951 mA/cm<sup>2</sup> to 6.092 mA/cm<sup>2</sup> and V<sub>oc</sub> from 0.573V to 0.703V for DSSCs sensitized with natural dyes. The best performance was obtained for the DSSC sensitized with Ziziphus jujuba with parameter J<sub>sc</sub> of 2.671 mA/cm<sup>2</sup>, V<sub>oc</sub> of 0.646 V, and an efficiency of 1.156% [3]. Islam M. Radwan found that the pre-treatment of the FTO with H<sub>3</sub>PO<sub>4</sub> and the post-treatment of TiO<sub>2</sub> with HNO<sub>3</sub> resulted in improved efficiencies of 130% and 250% respectively for the DSSCs sensitized by purple carrot [23].

### **1.9. Aim of this work**

In this thesis, DSSCs will be fabricated using TiO<sub>2</sub> as a semiconducting layer dyed with natural dyes extracted from flowers. Thin films of nanocrystalline TiO<sub>2</sub> will be prepared on transparent named Fluorine-doped tin oxide (FTO) coated glass using doctor blade method. Three natural dyes were used such as Hibiscus Sabdariffa, Rosa Damascena and Hibiscus Rosa Sinensis. The absorption spectra of these dyes will be performed. Different factors will be examined such as (pH of dyes, effect of some acids on TiO<sub>2</sub> and FTO by using pre-treatment and post-treatment, effect of ZnCl<sub>2</sub> dissoluble as a layer above TiO<sub>2</sub>). The J-V characteristic curves of all fabricated cells will be measured and analyzed. All DSSC parameters such as short circuit current density (I<sub>sc</sub>), open circuit potential (V<sub>oc</sub>), optimum current (I<sub>m</sub>), optimum voltage (V<sub>m</sub>), conversion efficiency (η), and fill factor (FF) will be calculated. Optimization of the fabricated cells with the best dye will be performed.

## Chapter Two

### Dye-Sensitized Solar Cells (DSSC)

In this chapter, the materials used to fabricate DSSCs and the cell parameters such as short circuit current  $J_{sc}$ , open circuit voltage  $V_{oc}$ , optimum current  $I_m$ , optimum voltage  $V_m$ , fill factor and efficiency are explained. The principal of operation of DSSCs are presented in details.

#### 2.1. Introduction

DSSC was developed by Grätzel in 1991 which was called "Grätzel Cell". This type of solar cells was classified as the third-generation of photovoltaic devices for the conversion of visible light to electric energy. The principle of operation of DSSCs depends on the photosensitization produced by the dyes adsorbed on the film surface of porous semiconductor material, and the sensitization produced by the dye absorption at portion of visible light spectrum.

#### 2.2. Materials of a dye-sensitized solar cell

##### 2.2.1. Substrates

DSSC electrodes as usually are prepared from transparent conducting oxide (TCO) coated glass substrate. Fluorine-doped tin oxide ( $\text{SnO}_2:\text{F}$ ) is a famous electrode of the standard DSSC. The main tasks of the conducting coating are collection of a current, support the structure of the cell and as a sealing layer between the cell and ambient air [17]. The choice of ( $\text{SnO}_2:\text{F}$ ) is due to the stability at a high temperatures where the standard preparation procedure of the nanostructured  $\text{TiO}_2$  electrode includes sintering of the deposited  $\text{TiO}_2$  film at 450-500 °C. An efficient DSSC substrate must have low sheet resistance that is independent on temperature, high transparency, and capability to forbid impurities from entering into the cell [24].

##### 2.2.2. Nanoparticle electrodes

The large band gap ( $>3$  eV) of the semiconducting oxides is very important in DSSCs for the transparency of the semiconductor electrode for the large part of the solar spectrum. The stable oxide semiconductors cannot absorb visible light because they have relatively wide gaps. Sensitization of wide band gap oxide semiconductor as  $\text{TiO}_2$  takes place with photosensitizers as natural dye where it can absorb visible light [25].  $\text{TiO}_2$  is a wide band gap ( $E_g \approx 3.2$  eV) semiconductor and has three

crystalline structures: anatase, rutile and brookite. Anatase is dominant in low temperatures (<800 °C) and has some properties of the most important, such as molar mass: 79.86 g/mol, melting point 1843 °C, boiling point 2972 °C, refractive index: 2.488 and density of 3.78 g/cm<sup>3</sup>.

TiO<sub>2</sub> has many advantages including high photosensitivity, high structure stability under solar irradiation and in solutions, non-toxic, and low cost. Nanoparticles of TiO<sub>2</sub> semiconductor is used to form a porous layer so that it can provide a large surface area and a relatively high porosity possible to adsorb enough dye for efficient light harvesting and a relative high conversion efficiency.

### **2.2.3. Sensitizer dyes**

The use of natural dyes as photosensitizers for the conversion of solar energy into electricity is interesting because, on one hand it enhances the economical aspect and, on the other, it has significant benefits from the environmental point of view [26]. There are some properties that must be available of the dye molecule as attached to the semiconductor particle surface to achieve a high light-to-energy conversion efficiency in the DSSC. The properties of the dye can be summarized as:

- The dye should have good adsorption onto the surface of semiconductor and not be desorbed by the electrolyte.
- Dye should be high soluble in some solvents used in the dye impregnation.
- Dye must absorb the light in the spectrum of the solar radiation. In DSSC, light must be only absorbed by dye molecules. The other layers (semiconductor or electrolyte) should not absorb the light.
- Excited state energy of the dye must be slightly over the TiO<sub>2</sub> conduction band and the energy difference must be sufficient to permit the transfer of electrons. Also, ground state energy level of the dye must be slightly below the reduction-oxidation potential of the electrolyte. This is necessary to obtain photo-voltage (conversion of solar energy to the electric energy) in a high level and maintain a minimum level of energy losses.
- The conduction band edge of the TiO<sub>2</sub> lie under the excited state of the dye to cause fast electron injection.
- The dye adsorbed TiO<sub>2</sub> surface must be stable for a long time in the working conditions.

#### **2.2.4. Electrolytes**

The electrolyte function is to return the electrons of the dye to complete the close circuit. The common electrolyte consists of iodine ( $I^-$ ) and triiodide ( $I_3^-$ ) as a redox pair in a solvent with possibly other substances added to improve the properties of the electrolyte.

These properties can be summarized as follow [27]:

1. High diffusion coefficients in the solvent to enable efficient mass transport.
2. Absence of significant spectral characteristics in the visible region to prevent absorption of incident light in the electrolyte.
3. High stability of both the reduced and oxidized forms of the couple to enable long operating life.
4. Highly reversible couple to facilitate fast electron transfer kinetics.
5. Chemically inert toward all other components in the DSSC.

The criteria for a suitable solvent for a high efficiency liquid electrolytes can be read as follows [28]:

1. The solvent must be liquid with low volatility at the operating temperatures ( $-40^\circ\text{C}$  -  $80^\circ\text{C}$ ) to avoid freezing or expansion of the electrolyte, which would damage the DSSCs.
2. It should have low viscosity to permit the rapid diffusion of charge carriers.
3. The intended redox couple should be soluble in the solvent.
4. It should have a high dielectric constant to facilitate dissolution of the redox couple.
5. The sensitizing dye should not desorb into the solvent.
6. It must be resistant to decomposition over long periods of time.
7. And finally from the point of view of commercial production, the solvent should be of low cost and low toxicity.

#### **2.2.5. Counter-electrode catalysts**

On the back of the DSSC there presents another glass substrate covered with a thin layer of Pt (Platinum) used as the catalyst to regenerate  $I^-$  and as the cathode material. The function of the counter electrode is to transfer the electrons arriving from the external circuit back to the redox electrolyte. Pt is the best material to make efficient

devices technically. But considering high expenses, carbon cathode has been an ideal substitute, such as carbon black, carbon nanotubes etc. In 2006, Gratzel's group employed carbon black as the material of counter electrode, and reaches an efficiency of 9.1%, which is 83% of that using Pt [29].

Conducting polymers can also be used. Polyaniline film on stainless steel by electrochemical polymerization has been reported as a counter electrode of DSSC. It is cheap and non-fragile [30,31].

### 2.2.6. Sealing

The space between the photo electrode and the counter electrode are filled with a liquid type electrolyte for electron transfer into the cell. Therefore, an appropriate sealing method is required to prevent the liquid electrolyte leaking out. The sealing technique improves the durability and stability of the DSSCs. The optimal conditions for the sealing of the DSSCs are related to the pin-hole diameter, the discharge current and the moving velocity of the target [32]. In addition, it prevents leakage. Sealing must be impervious to water vapor and ambient air, chemically inert towards the electrolyte and other cell components and coalesce well to the glass substrate and TCO coating.

### 2.3. Operating principle

The operation of a DSSC is shown in Fig. 2.1. Photons are converted into an electric current by charge injection of excited dye molecules into a wide band gap semiconductor [34]. A photon is absorbed by the dye molecule and this leads to excite the dye to an electronically excited state ( $S^*$ ):



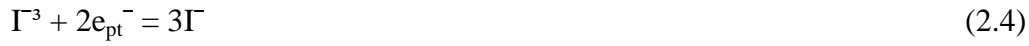
The excited electrons are injected by excited dye molecule into the conduction band of stable semiconductor ( $TiO_2$  electrode) and the dye becomes oxidized ( $S^+$ ):



The original state of the dye ( $S$ ) is subsequently restored by the electron from the electrolyte through the reduction of iodide:



The regeneration of dye from iodide prevents the capture of the conduction band electrons through the dye oxidation. The iodide is in turn regenerated at the counter electrode by reducing tri-iodide as follows:



The electrical cycle is completed where the electron flows through the outer electrical circuit and performs work.

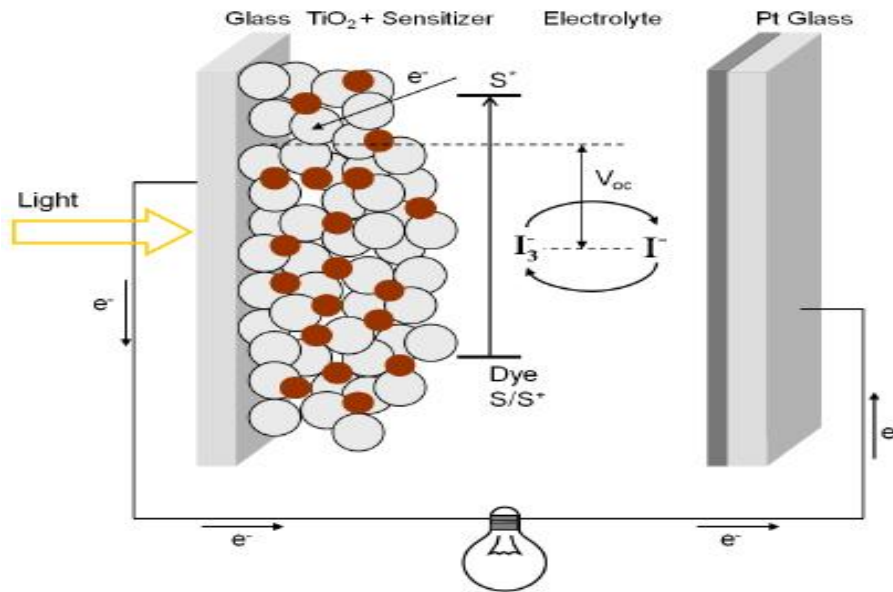


**Fig. 2.1** The working principle of dye-sensitized nanostructure solar cell.

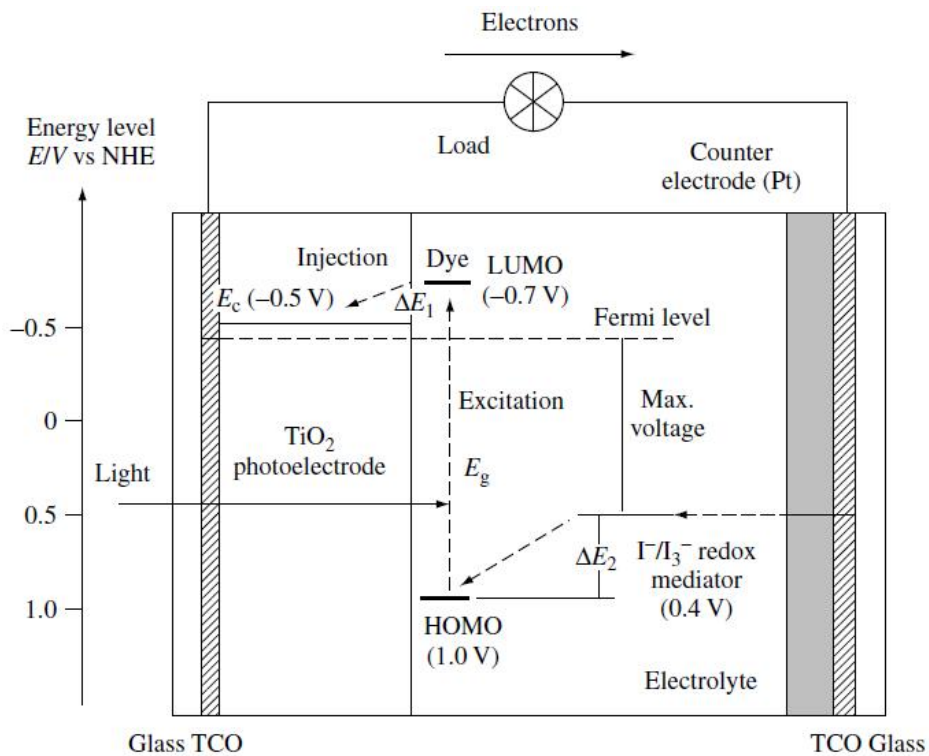


**Fig. 2.2** Schematic energy diagram

The performance of a DSSC is predominantly based on four energy levels of the component: the excited state (approximately LUMO) and the ground state (HOMO)

of the photosensitizer, the Fermi level of the TiO<sub>2</sub> electrode, which is located near the conduction-band level, and the redox potential of the mediator (Γ/Γ<sup>3</sup>) in the electrolyte.

The photocurrent obtained from a DSSC is determined by the energy difference between the HOMO and the LUMO of the photosensitizer, analogous to the band gap,  $E_g$ , for inorganic semiconductor materials. The smaller the HOMO–LUMO energy gap, the larger the photocurrent will be because of the utilization of the long-wavelength region in the solar spectrum. The energy gap between the LUMO level and the conduction-band level of TiO<sub>2</sub>,  $\Delta E_1$ , is important, and the energy level of the LUMO must be sufficiently negative with respect to the conduction band of TiO<sub>2</sub> to inject electrons effectively. In addition, substantial electronic coupling between the LUMO and the conduction band of TiO<sub>2</sub> also leads to effective electron injection. The HOMO level of the complex must be sufficiently more positive than the redox potential of the Γ/Γ<sup>3</sup> redox mediator to accept electrons effectively ( $\Delta E_2$ ) [35].

## **2.4. Parameters of solar cells**

In this section the most important parameters such as short circuit current ( $J_{sc}$ ), open circuit voltage ( $V_{oc}$ ), optimum current ( $I_m$ ), optimum voltage ( $V_m$ ), fill factor (FF) and efficiency ( $\eta$ ) are presented.

### **2.4.1. Short circuit current density $J_{sc}$**

This current appears when the potential difference across the cell equals to zero, where it called short circuit cell  $J_{sc}$  as shown in Fig. 2.3.  $J_{sc}$  is equal to the absolute number of photons converted to the hole-electron pairs. It depends on the solar cell structure, material properties, and the operating conditions [35].

### **2.4.2. Open circuit potential $V_{oc}$**

If the output current is zero, the cell is open circuited and the voltage of the cell is called open circuit voltage. It depends on both the Fermi level of the semiconductor and the level of dark current [23]. The theoretical maximum of the  $V_{oc}$  of the cell is determined by the difference between the Fermi level of the semiconductor and the redox potential of the electrolyte.

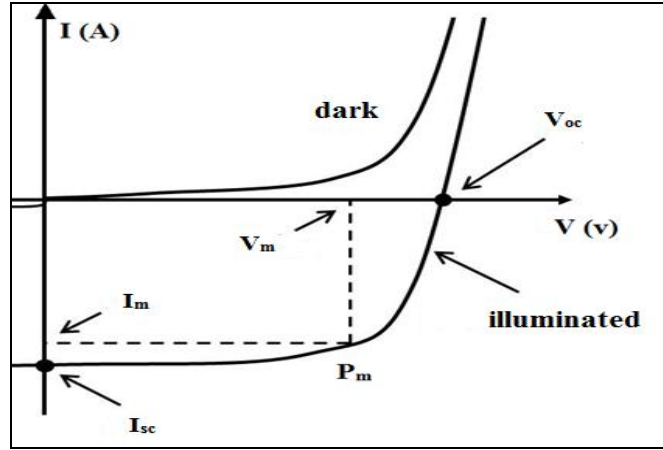


**Fig. 2.3** Typical J-V curve of a solar cell showing the open circuit voltage  $V_{oc}$ , short circuit current  $I_{sc}$ , and the maximum power point  $P_m$  [23].

### 2.4.3. Optimum voltage $V_m$

$V_m$  is the voltage at the optimum operating point (as shown in Fig. 2.3) at which the DSSC output power is maximum. It depends on bonds between the dye molecule and  $TiO_2$  film [3].

### 2.4.4. Optimum current density $J_m$

$J_m$  is the current at the optimum operating point (as shown in Fig. 2.3) at which the DSSC output power is maximum.

### 2.4.5. Fill factor

The ratio of peak output  $V_m J_m$  to  $V_{oc} J_{sc}$  is called fill factor (FF) of a solar cell. Mathematical formula for this concept is [6]:

$$FF = \frac{V_m J_m}{V_{oc} J_{sc}} \quad (2.5)$$

Where

$$P_m = V_m J_m \quad (2.6)$$

where  $P_m$  is the maximum optimal power output. The meaning of fill factor can be understood from its graphical representation. It indicates how much area underneath the J-V characteristic curve is filled by the rectangle described by  $V_m J_m$  (as shown in Fig. 2.3) in relation to the rectangle  $V_{oc} J_{sc}$ . The theoretically maximum obtainable FF is a function of the open circuit potential. Fill factors for optimized solar cells are typically within the range of 0.6–0.75.

### 2.4.6. Efficiency $\eta$

The ratio of output electrical power of the solar cell and the power of incident light  $P_{(in)}$  is called the conversion of energy or efficiency. The value of  $P_{(in)}$  at the earth ground is approximately  $100 \text{ mW/cm}^2$ . The maximum efficiency can be calculated from the J-V curve according to the relation:

$$\eta = \frac{FF \cdot J_{sc} V_{oc}}{P_{(in)}} \quad (2.7)$$

$J_{sc}$  is directly proportional to the incident optical power  $P_{(in)}$  while  $V_{oc}$  increases logarithmically with the incident power so the overall efficiency of solar cell is expected to increase logarithmically with incident power [32]. The temperature of the cell and the quality of the illumination are very effective to obtain high efficiency, so there is a standard conditions used in different laboratories, taking light intensity equals  $100 \text{ mW/cm}^2$ , Air Mass 1.5 spectrum and a temperature cell of  $25^\circ\text{C}$ .

### 2.4.7. The simple electrical model of a solar cell

A simple equivalent circuit corresponding to a solar cell is shown in Fig. 2.4 [3]. A solar cell can be thought as a combination of a current source and diode in the solar cell having series resistance ( $R_s$ ) and shunt resistance ( $R_{sh}$ ). The cell would be an ideal cell if  $R_s$  is zero, and  $R_{sh}$  is infinitely large. In fact this is not a practical case.

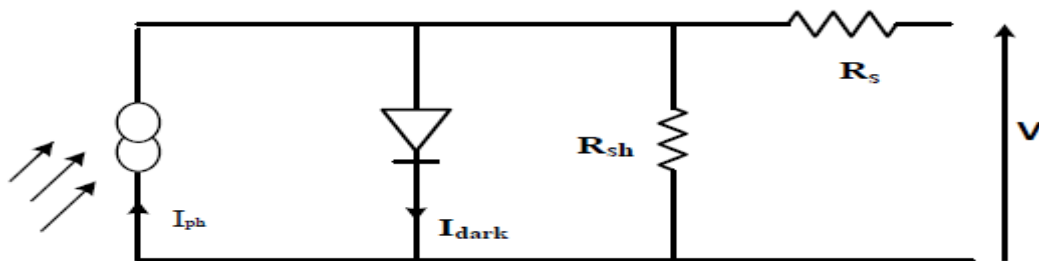


**Fig. 2.4** Equivalent circuit of a solar cell including series and shunt resistances.

The  $R_s$  is composed of the electric resistance of different materials in the cell and interfaces between them. The resistance of the TCO layer has the biggest influence on the series resistance. The shunt resistance measures the resistance between the electrodes of the cell through undesirable routes for example from  $\text{TiO}_2$  film to electrolyte. It is desired to be as high as possible. The diode model does not represent the dye solar cell very well. The internal structure of the DSSC is more complex than

that of silicon solar cell. But the concepts of the series and parallel resistances can also be applied to the DSSC. The resistance can be measured using impedance spectroscopy. Series and parallel resistances have a considerable effect on the fill factor as shown in Fig. 2.5. For an efficient cell we need  $R_s$  to be as small and  $R_{sh}$  to be as large as possible.

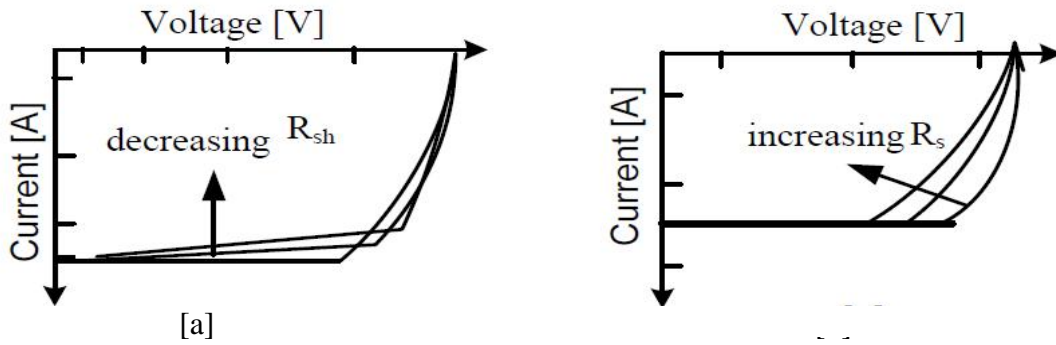


**Fig. 2.5** Effect of (a) reducing parallel resistance and (b) increasing series resistance.

The effect of  $R_s$  and  $R_{sh}$  is shown in Fig. 2.5. The effect of decreasing  $R_{sh}$  and increasing  $R_s$  is to reduce the area of the maximum power rectangle compared to that with area  $J_{sc}$  cross  $V_{oc}$ .

## Chapter Three

### Description of Instruments and Techniques of Fabrication of DSSC

In this chapter, materials and techniques used for the preparation of DSSC are discussed. Instruments used to fabricate and characterize the cells are described.

#### 3.1. Materials used in the preparation of DSSCs

1. A Nanoparticle material ( $\text{TiO}_2$ ) as a semiconductor layers named P25.
2. Fluorine-doped tin oxide ( $\text{SnO}_2 : \text{F}$ ) as a conductive glass plate.
3. Natural dyes extracted from flowers coronets as listed in Table 3.1.
4. A counter electrode fabricated from FTO-coated glass, coated with of platinum catalyst layer.
5. A redox ( $\Gamma / \Gamma^3$ ) electrolyte solution.
6. Electrical contact between working and counter electrodes is achieved using alligator clips.

#### 3.2. Experimental

##### 3.2.1. Extraction of natural dyes

Flowers were collected from three plants (tabulated in Table 3.1) and the coronets of the flower were used. These coronets were first washed by distilled water, dried at  $60^\circ\text{C}$  and then 15g of each of the dried natural coronet were immersed in 10 ml of ethyl alcohol at room temperature and in the dark for 24 hours. After filtration of the solutions, natural dyes were obtained.

##### 3.2.1.1. Measuring absorption spectra of natural dyes

The absorption spectra measurements of the extracted dyes (Hibiscus Sabdariffa; Hibiscus Rosa Sinensis and Rosa Damascena) in ethyl alcohol solution were performed using a UV-Vis spectrophotometer (400 to 800 nm).

**Table 3.1** Flowers used in this study to extract the natural dyes.

No.	Name of flower	Name in Arabic
FD.1	Hibiscus Rosa Sinensis	زهرة الفونوغراف (أحمر اللون)
FD.2	Rosa Damascena	زهرة الجوري (أحمر اللون)
FD.3	Hibiscus Sabdariffa	زهرة الكركديه (أحمر اللون)

### 3.2.2. FTO cleaning

The conductive glass substrates Fluorine doped tin oxide (FTO) were cut into pieces with area of 2.56 cm<sup>2</sup> with dimensions of 1.6 cm × 1.6 cm. The substrates were cleaned in a detergent solution using an ultrasonic bath for 20 minutes twice, then immersing in boiling water for 30 minutes to get more cleaned, rinsed with distilled water and ethanol, then dried for 20 minutes and kept in an oven at 60 °C. The sheet resistance of the (FTO) was measured and found to be 17-23 Ω/sq.

### 3.2.3. Preparing of TiO<sub>2</sub> film

The TiO<sub>2</sub> paste was prepared by adding of 2g of TiO<sub>2</sub> nanopowder of (10-25nm) in size (type P25), 4 ml distilled water, 10 μl acetyl acetone and 50 μl Triton X-100, then grinding the mixture for half an hour until a homogeneous paste was obtained. The TiO<sub>2</sub> paste was distributed on the glass substrates using doctor blade method. To make thin films; two pieces of tape with thickness 20 μm were used as shown in the Fig. 3.1. After the paste was spread, the films were left to dry for 5 min. before removing the tape, and placing them in an oven at 70 °C for 30 min. and left to dry. The required area of 0.25 cm<sup>2</sup> with dimensions of 0.5 cm × 0.5 cm was taken.

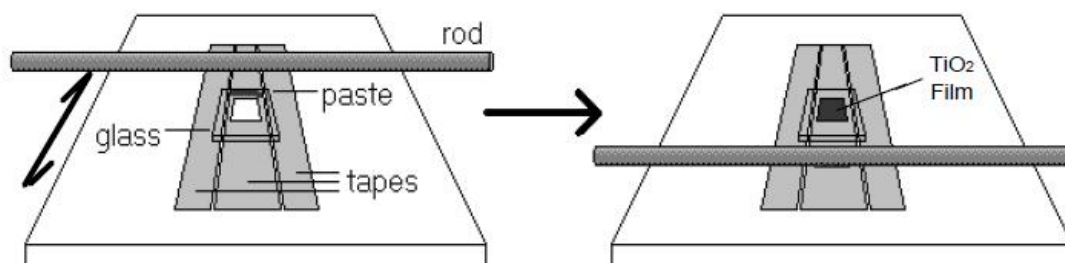


**Fig. 3.1** Doctor blade method to spread the TiO<sub>2</sub> paste on the FTO coated glass.

### 3.2.4. Sintering of TiO<sub>2</sub> and DSSC assembly

The films were sintered at 450 °C for 30 minutes and then were cooled down to about 100 °C to cause more adhesion between TiO<sub>2</sub> and dye molecule. The sintered films were dyed for 24 hour under dark. The dyed TiO<sub>2</sub> electrode and platinum counter electrode were assembled to form a solar cell by sandwiching a redox ( $\Gamma/\Gamma^3$ ) electrolyte solution which is composed of 2ml acetonitrile (ACN), 8 ml propylene carbonate (p-carbonate), 0.668 gm (KI), and 0.0634 gm (I<sub>2</sub>).

It is worth mentioning that the previous steps are fixed for all what has been accomplished in the laboratory and some other factors were changed such as changing

the pH value of the dye solution or increase the acidic surface of titanium dioxide; which will be presented in detail.

### **3.3. Techniques used to improve the Efficiency**

Four experiments were conducted, namely treating the FTO substrate and TiO<sub>2</sub> layers with three acids, such that pH of the dye solutions, and coating TiO<sub>2</sub> particle with Zinc Oxide layer.

#### **3.3.1. FTO acidic treatment**

The FTO layers were cleaned carefully using ultrasonic bath for 20 minutes twice, then immersing in boiling water for 30 minutes, rinsed with distilled water and ethanol, then dried in an oven at 60 °C for 20 minutes. The cleaned FTO were immersed in diluted acids hydrochloric acid, nitric acid, and phosphoric acid for five and ten minutes. A 0.1 M from each acid was prepared. The TiO<sub>2</sub> past was spread onto acidic pre-treatment FTO layers then sintered then dyed for 24 hour under dark.

#### **3.3.2. TiO<sub>2</sub> film acidic treatment**

The sintered TiO<sub>2</sub> films were immersed in diluted acids for five minutes then washed by distilled water for 30 minutes in an oven at 60 °C before dying process. The acidic treated films were dyed for 24 hour under dark then the process of the DSSC fabrication was done as mentioned before.

#### **3.3.3. Effect of changing pH of dye solutions.**

The pH of the natural dye extracts were measured using pH meter without any additions and found to be 6.65 for Hibiscus Rosa Sinensis, 6.15 for Rosa Damascena, and 3.23 for Hibiscus Sabdariffa. A 0.1 molar concentration of hydrochloric acid and acetic acid were prepared by adding drops of dilute solutions of acids to dye solutions to change the values of the pH. The TiO<sub>2</sub> film were dyed for 24 hour under dark by different pH dye solutions.

#### **3.3.4. Successive ionic layer absorption and reaction method.**

The successive ionic layer absorption and reaction method (SILAR) is used to create coatings on thin films for technological products such as photovoltaic cells. By allowing thin films to be coated in different chemicals at or close to room temperature, metallic films or films incorporating metallic parts can use the SILAR

method and avoid possible problems with damage caused by oxidation or corrosion. Other methods of thin film deposition use the transfer of atoms to provide a coating over thin films. The SILAR method uses the transfer of ions that provides better coverage of chemicals over the film, and can result in a finer grain structure than other deposition methods. One of the advantages of the SILAR method of coating thin films is the number of different materials that can be used to create a film for a desired application. Materials that can be used in the method include temperature sensitive substrates such as polyester because the SILAR method is completed at or close to room temperature. The thin film production method known as SILAR requires the film to be immersed in the chemicals required for creating a chemical solution over the substrate. Between each immersion of the film into the chemicals, the film is rinsed using purified water to create the desired coating over the film. The main advantages of the SILAR deposition method include the ease of completing the method and the relative low cost. For small amounts of substrates to be treated using the SILAR method, the process can be completed using glass beakers [35,36].

In this thesis, three solutions of Zinc Chloride with different molar concentrations were prepared (0.1M, 0.05M, 0.01M). Ammonium hydroxide were added to the different zinc chloride solutions and then white precipitate was formed. The white precipitate must be dissolved in the zinc chloride solutions by adding more ammonium hydroxide until Zinc Ammonium complex is formed as shown in Eq. 3.1:



TiO<sub>2</sub> film was immersed into the solution for 15 seconds after heating the film to a temperature of 100°C. The TiO<sub>2</sub> film directly was submerged in boiling water at temperature 90°C for 30 seconds to form ZnO layer. The samples were dyed for 24 hour under dark then taken to carry out the measurement.

### **3.4. Description of instruments**

#### **3.4.1. Autolab PGSTAT 302N**

The Autolab PGSTAT 302N instrument manufactured by Metrohm Autolab company as shown in Fig. 3.2. It is an electrochemistry instrument, that uses NOVA program as a control software. Any cell or electrochemical interface can be described in terms of an electric circuit, to determine the resistive, capacitive and inductive behavior of the cell at that particular frequency [37,38].



**Fig. 3.2** The Autolab PGSTAT 302N instrument with frequency response analyzer of Module (FRA 32).

Electrochemical impedance spectroscopy (EIS) measurements can be performed with the Autolab instruments in combination with the Frequency response analyzer (FRA). In a typical electrochemical impedance measurement, the FRA module generates a sine wave with a user-defined frequency and a small amplitude. This signal is superimposed on the applied DC potential or current of the cell. The AC voltage and current components are analyzed by the two FRA channels and the transfer function. The total impedance  $Z$  is calculated, together with the phase angle shift and the real and imaginary components of the total impedance. If the real part  $\{\text{Re}(Z)\}$  is plotted on the X-axis and the imaginary part  $\{-\text{Im}(Z)\}$  is plotted on the Y-axis of a chart, we get a "Nyquist Plot" is obtained as shown in Fig. 3.3. In this plot the Y-axis is negative and each point on the Nyquist Plot is the impedance at one frequency. Fig. 3.3 has been annotated to show that low frequency ( $\omega=0$ ) data are on the right side of the plot and higher frequencies ( $\omega \approx \infty$ ) are on the left.

On the Nyquist Plot the impedance can be represented as a vector (arrow) of length  $|Z|$ . The angle between this vector and the X-axis, is called the phase angle ( $\phi$ ).

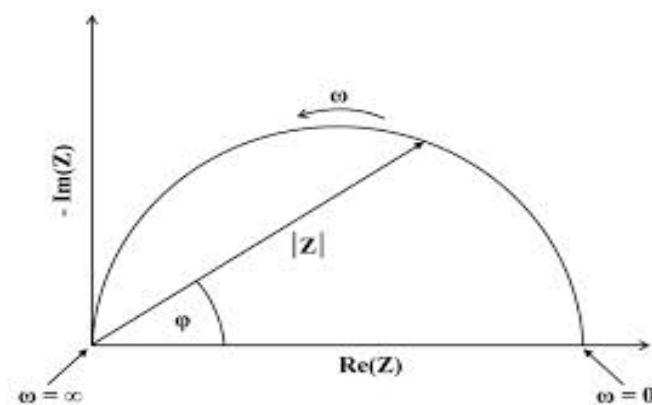


**Fig. 3.3** Nyquist Plots

Nyquist Plots have one major shortcoming. Any data point on the plot, cannot tell what frequency was used to record that point. The semicircle is characteristic of a single "time constant". From the DSSC, Electrochemical impedance plots often contain three semicircles; the first semicircle represent the FTO glass substrate, the second represent the TiO<sub>2</sub> film and the third represent the dye molecule layer.

Another popular presentation method is the Bode Plot. The impedance is plotted with log frequency on the X-axis and both the absolute values of the impedance ( $|Z|=Z_0$ ) and the phase-shift on the Y-axis.

The Bode Plot is shown in Fig. 3.4. Unlike the Nyquist Plot, the Bode Plot does show frequency information.

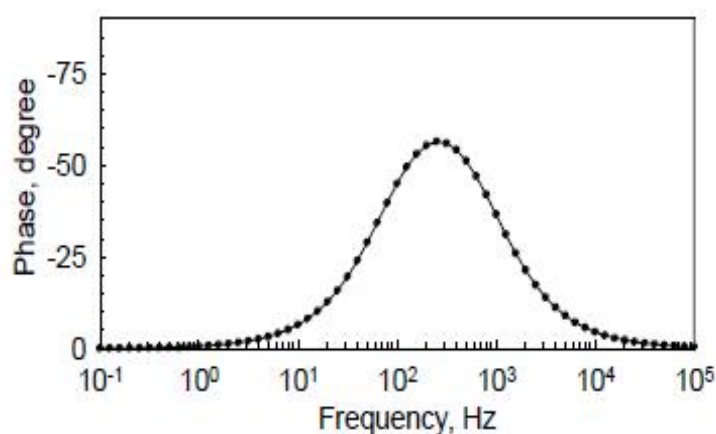


**Fig. 3.4** Bode plot showing the phase angle as a function of frequency

DSSC can be described in terms of an electric circuit, which is a combination of resistances, capacitances and inductances. If such an electric circuit produces the same response as the cell does when the same excitation signal is imposed, it is called the equivalent electric circuit of the cell. The equivalent circuit should be as simple as possible to represent the system targeted [37,39]. EIS can establish a hypothesis using equivalent circuit models. A data-fitted equivalent circuit model will suggest valuable chemical processes for the electrochemical system being studied.

In this work, EIS was measured for three cells using Autolab PGSTAT 302N with frequency response analyzer FRA 32 Module. After analyzing the results, the equivalent circuit for each cell was found. The cells were prepared using Hibiscus Rosa Sinensis dye as a sensitizer. The AC amplitude were taken as -0.4 v, -0.6 v and -0.8 v for all cells under dark and illuminated conditions for all measurements. All the

measurements were carried out with the NOVA software. The impedance was measured and plotted to obtain Nyquist and Bode plots.

### **3.4.2. Ultraviolet and visible absorption spectroscopy (UV-Vis).**

Ultraviolet-Visible (UV-Vis) spectroscopy is used to obtain the absorbance spectra of a compound in a solution or as a solid. It is the measurement of a beam of light after its reflection from a surface of a sample or passing through it. The UV-Vis spectrometer consists of light source, monochromator with diffraction grating, sample holder and detector. In this work, the absorption spectra were recorded by Genesys 10S UV-Vis spectrophotometer with code L9M3130012 and a range of measurement from 400 nm to 800 nm was adopted. This device is manufactured by Thermo Scientific company as shown in Fig. 3.5. It is designed specifically for researchers in the fields of molecular biology, biochemistry, and other life science disciplines [40,41].



**Fig. 3.5** Genesys 10S UV-Vis spectrophotometer

### **3.4.3. J-V measurement set up.**

A solar simulator is usually used in solar cell performance measurements because solar radiation is not always available and the intensity of radiation varies from one area to another and from time to another.

An J-V measurement system measures J-V curves of solar cells to obtain  $V_{oc}$  and  $J_{sc}$  and to calculate critical cell performance parameters including fill factor (FF), maximum current ( $I_m$ ), maximum voltage ( $V_m$ ), maximum power ( $P_m$ ), and efficiency ( $\eta$ ). The system used in this work is shown in Fig. 3.6. It consists of light source (a high pressure mercury arc lamp with IR filter), computer, the measurement electronics, and Labview program as a software to measure DSSC J-V curves. A voltage from -1 to 1 volt applied to the cells where the resulting current and voltage are measured using NI USB6251 data acquisition card in combination of a Labview program.



**Fig. 3.6** System of I-V measurement and solar cell simulator

#### **3.4.4. Diffuse reflectance and Kubelka-Munk.**

When infrared radiation is directed onto the surface of a solid sample, two types of reflection can occur: specular reflection and diffuse reflection. The specular component is the radiation that reflects directly off the sample surface according to the normal reflection law; angle of reflection equals angle of incidence as shown in Fig. 3.7. Diffuse reflection is the radiation that penetrates into the sample and then emerges at all angles after suffering multiple reflections and refractions by the sample particles as shown in Fig. 3.8. A diffuse reflection accessory is designed so the diffusely reflected energy is optimized and the specular component is minimized. The optical system collects the scattered radiation and directs it to the infrared detector.

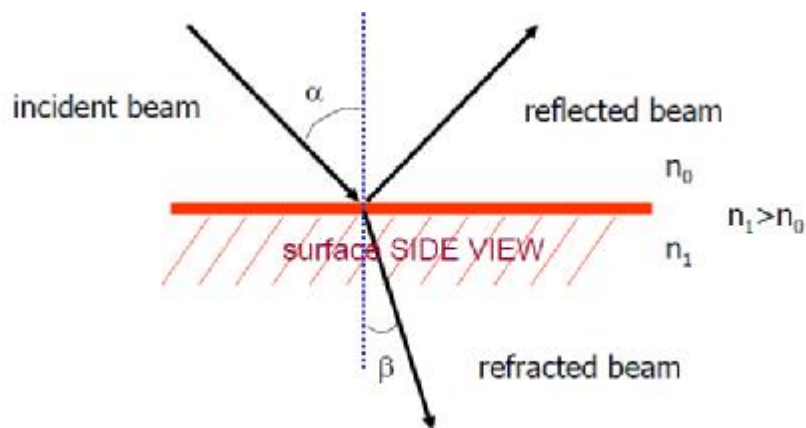


**Fig. 3.7** Specular reflection diagram

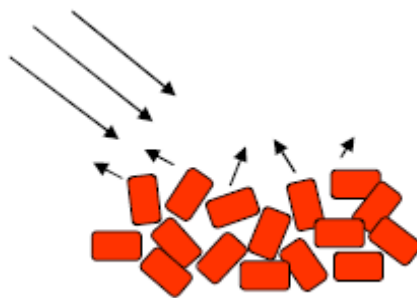


**Fig. 3.8** Diffuse reflection diagram

A theory of diffuse reflection at scattering surfaces was derived by Munk in 1931 and Kubelka 1948 describes optical characteristics (e.g. reflectance, transmittance and absorptance). The Kubelka-Munk model relates sample concentration to the intensity of the measured infrared spectrum.

The Kubelka -Munk function is given as [42]:

$$F(R) = \frac{(1-R)^2}{2R} = \frac{K}{S} \quad (3.2)$$

where:

R = absolute reflectance of the layer

K= molar absorption coefficient

S= scattering coefficient

The diffuse reflection spectra were collected then transformed to the absorption spectra at the wavelength range of 200 – 800 nm with a Evolution 220 UV-Visible spectrophotometer instrument with ISA-220 Integrating Sphere Accessory manufactured by Thermo Scientific company as shown in Fig. 3.9. The absorption spectra were obtained and plotted their values on Y-axis vs. the wavelength that plotted on X-axis.



**Fig. 3.9** Evolution 220 UV-Visible spectrophotometer instrument with ISA-220 Integrating Sphere Accessory [43].

## Chapter Four

### Results And Discussion

In this chapter, the absorption spectra of the dyes are presented. The J-V characteristic curves of the fabricated cells are studied. The output power is plotted versus the voltage of the cell. Short circuit current  $J_{sc}$ , open circuit voltage  $V_{oc}$ , fill factor FF, and power conversion efficiency  $\eta$  are all presented.

#### 4.1. Sensitization of DSSCs by three plant flowers

##### 4.1.1. Absorption spectra of the extracts

A GENESYS 10S UV-Vis spectrophotometer was used to measure the absorption spectra of the dye solutions extracted from dried flowers. The wavelength range of absorption spectra analysis was taken from 400 to 800 nm. Fig. 4.1 shows the UV-Vis absorption spectra of the natural dyes extracted from the flowers of Hibiscus Rosa Sinensis, Hibiscus Sabdariffa, and Rosa Damascena.

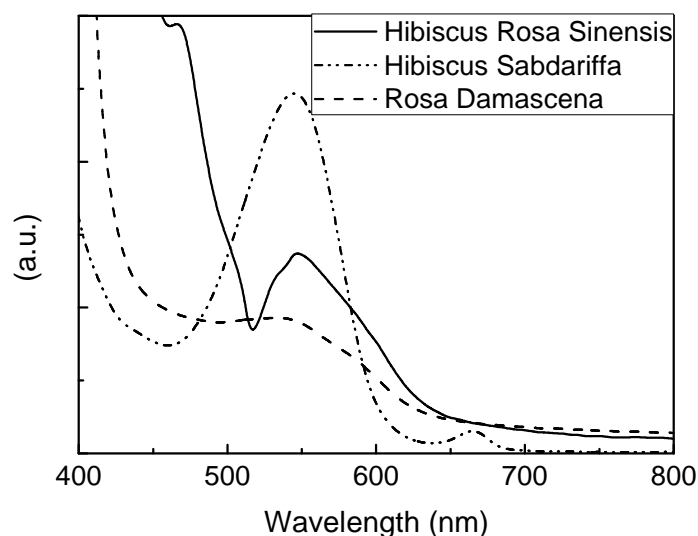


**Fig. 4.1.** The UV-Vis absorption spectra of the dyes extracted from Hibiscus Rosa Sinensis, Hibiscus Sabdariffa, and Rosa Damascena.

The absorption spectra of the extracts showed the presence of distinct absorption peaks in the visible region. The absorption peaks of Hibiscus Sabdariffa dye can be seen at about 545 nm and 664 nm. The absorption peak of Rosa Damascena dye is at 541.63 nm and those of Hibiscus Rosa Sinensis dye are at 442 nm and 548 nm. It is found that the dye extracted from Hibiscus Rosa Sinensis has a wide absorption band

with peaks at about 548 nm and 440 nm. The absorption spectrum of Hibiscus Rosa Sinensis dye solution was in agreement with those reported by Fernando and Senadeera [44] for Hibiscus Rosa Sinensis dye that was extracted using acidified ethanol, which resulted in an absorption peak at 540 nm where the anthocyanin is the effective material that caused the peaks. The difference in the absorption characteristics resulted from the different types of functional groups on the anthocyanins and the colors of the extracts [44].

#### 4.1.2. Photovoltaic parameters

The J-V measurements of the DSSCs sensitized using the extracts of the three natural dyes are presented in Fig. 4.2. For each DSSC, the measured current density  $J$  versus the voltage  $V$  is presented at light intensity of  $100 \text{ mW/cm}^2$ . The power  $P$  is plotted versus the voltage for each DSSC as shown in Fig. 4.3. Through the study and analysis of these curves the cell parameters can be determined. The maximum power point is determined from the P-V curves from which  $J_m$  and  $V_m$  can be obtained. The fill factor and cell efficiency are calculated using Eq. (2.1) and Eq. (2.3). All the photovoltaic parameters of the fabricated DSSCs are listed in Table 4.1.

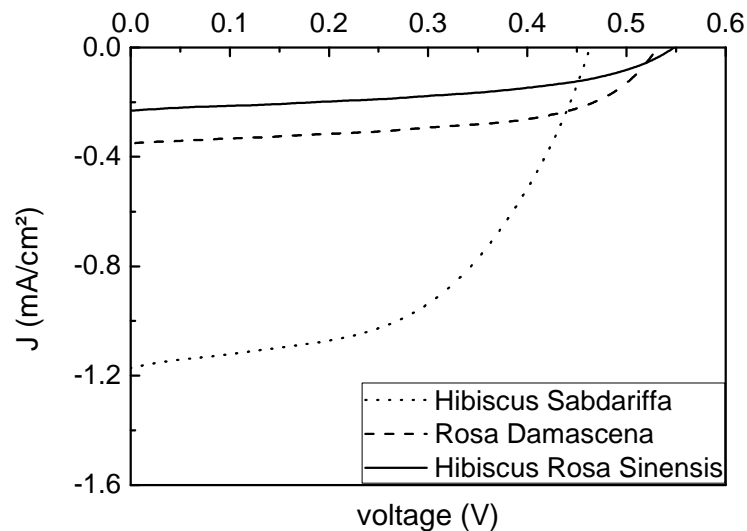


**Fig. 4.2.** Current density-voltage characteristics curves for the DSSCs sensitized by Hibiscus Sabdariffa, Hibiscus Rosa Sinensis, and Rosa Damascena.

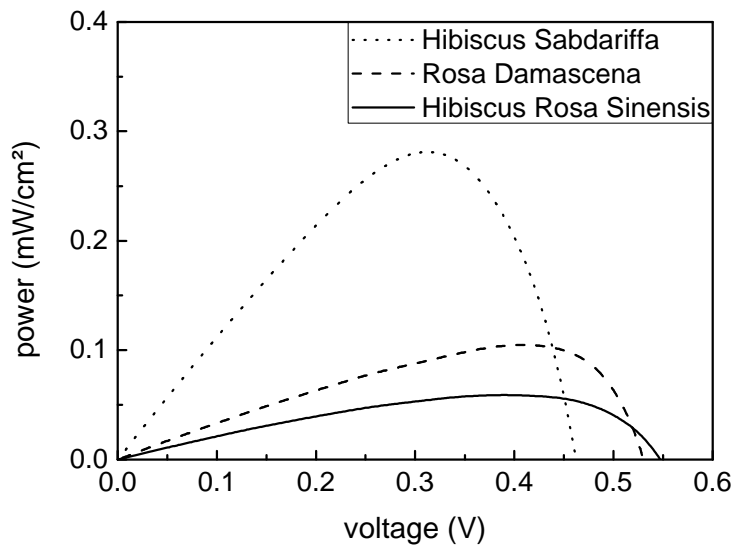


**Fig. 4.3.** Power-voltage characteristics curves for the DSSCs sensitized by Hibiscus Sabdariffa, Hibiscus Rosa Sinensis and Rosa Damascena.

**Table 4.1** Photovoltaic parameters of the DSSCs sensitized by the three natural dyes.

Dye	$V_{oc}$ (V)	$J_{sc}$ (mA/cm <sup>2</sup> )	$V_m$ (V)	$J_m$ (mA/cm <sup>2</sup> )	FF	$\eta$ %
Hibiscus Rosa Sinensis	0.55	0.23	0.41	0.15	0.49	0.06
Hibiscus Sabdariffa	0.46	1.18	0.32	0.89	0.51	0.28
Rosa Damascena	0.53	0.35	0.41	0.26	0.56	0.11

As shown in Table 4.1, the  $V_{oc}$  ranges between 0.46 V for DSSC sensitized with Hibiscus Sabdariffa extract and 0.53 V for the cell dyed with Rosa Damascena. The  $J_{sc}$  has a maximum value of 1.18 mA/cm<sup>2</sup> for the DSSC sensitized with the dye extracted from Hibiscus Sabdariffa, and a minimum value of 0.23 mA/cm<sup>2</sup> for the DSSC sensitized with the dye extracted from Hibiscus Rosa Sinensis. The fill factor of the fabricated cells ranges from 49% to 56%. The highest fill factor was obtained for the DSSC sensitized with the extract of Rosa Damascena and the lowest one was observed for the cell dyed with Hibiscus Rosa Sinensis. The highest efficiency has a value of 0.28% for the DSSC sensitized with Hibiscus Sabdariffa, while the lowest efficiency has a value of 0.06% for the DSSC sensitized with Hibiscus Rosa Sinensis.

The low fill factor may be caused from poor connection between material interfaces and low mobility of electrolyte [45]. Moreover, the resistance of  $\Gamma^3$  diffusion increases with decreasing the concentration of  $\Gamma^3$  leading to a lower FF [46]. The low values of efficiency in the fabricated DSSCs may be due to the fast charge recombination rate, lower electron transfer from the dye molecule to the conduction band of  $\text{TiO}_2$  or incompatibility between the conduction band edge of  $\text{TiO}_2$  and the energy of the excited state of the adsorbed dye [47].

According to Table 4.1 and Fig. 4.1, Hibiscus Sabdariffa dye showed the best efficiency according to the good photo-to-electric conversion that for high absorbance of photons, but when treatments were applied to improve the efficiency, to be presented later the efficiency was damped for all treatment processes whereas Hibiscus Rosa Sinensis showed the best efficiencies improvement after applying the treatments may be connected with large area of the absorption peak and faster injection of the electrons. So, Hibiscus Rosa Sinensis was chosen as a main sensitizer for further studies.

The Hibiscus Rosa Sinensis contains high content of anthocyanin pigments [44]. The advantage of anthocyanin is the binding of hydroxyl and carbonyl groups to the surface of the porous  $\text{TiO}_2$  film as shown in Fig. 4.4. This causes electron transfer from the anthocyanin molecule to the conduction band of  $\text{TiO}_2$ . The difference in the absorption characteristics resulted from the different types of functional groups on the anthocyanin and the colors of the extracts affected by the pH [48]. There are many colors of Hibiscus Rosa Sinensis dyes as red, yellow, violet, white and pink. The flowers used in this work were red colored as shown in Fig. 4.5.

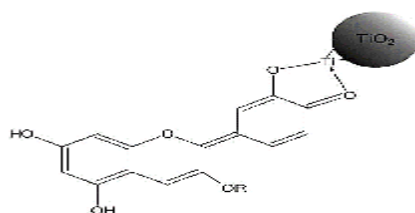


**Fig. 4.4.** Molecular structure of anthocyanin and the binding between anthocyanin molecule and  $\text{TiO}_2$  particles [23]



**Fig. 4.5.** Hibiscus Rosa Sinensis, Hibiscus Sabdariffa, and Rosa Damascena flowers.

According to the Kubelka-Munk relationship, the diffuse reflectance spectra were collected with a Evolution 220 UV-Visible spectrophotometer instrument with ISA-220 Integrating Sphere Accessory and transformed to the absorption spectra. Fig. 4.6 shows the absorption spectra of TiO<sub>2</sub> electrode after being dyed with Hibiscus Rosa Sinensis and that of the extract from Hibiscus Rosa Sinensis in ethanol.

The absorption spectrum for the extracted dye in ethanol shows a peak at wavelength of 548 nm where the absorption spectrum for that adsorbed onto TiO<sub>2</sub> film shows a wider one at a wavelength of 585 nm. This refers to the red shifted towards higher wavelength according to the bonding strength between anthocyanin and TiO<sub>2</sub> ions [49].

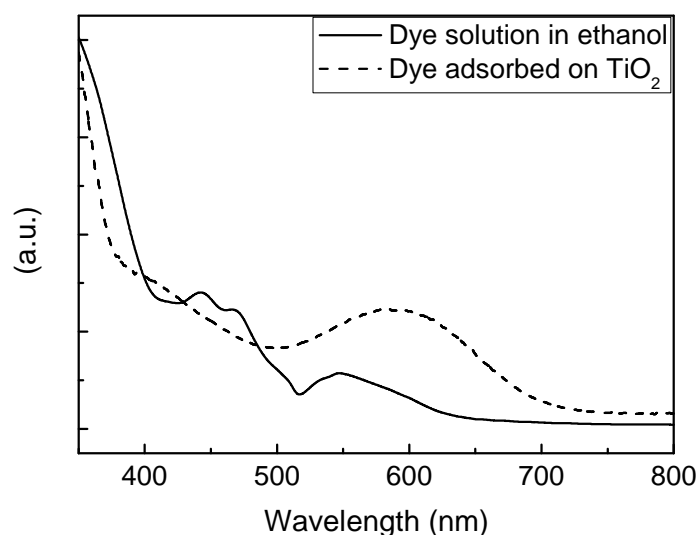


**Fig. 4.6.** Absorption spectra of Hibiscus Rosa Sinensis dye on TiO<sub>2</sub> film and the extract of the same flower in ethanol.

## 4.2. FTO acidic treatment

In this process, the FTO layer was pre-treated with hydrochloric (HCl), phosphoric ( $\text{H}_3\text{PO}_4$ ), and nitric acids ( $\text{HNO}_3$ ). The FTO substrates were immersed in 0.1M of one of the acids for 5 minutes and then washed by distilled water and dried in an oven at 60 °C for 30 minutes.  $\text{TiO}_2$  paste was distributed on the treated glass substrates using doctor blade method then dyed with dye solutions at room temperature for 24 hours and finally the DSSCs were assembled. The same steps of FTO acid pre-treatment were repeated for a time of immersion of 10 minutes.

### 4.2.1. J-V characterizations

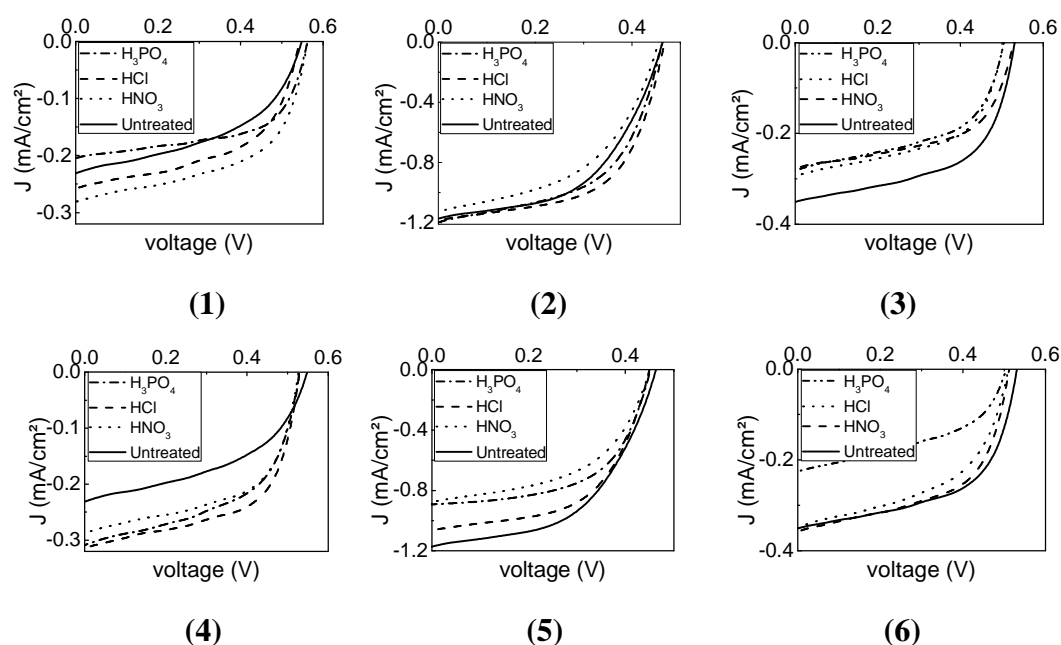


**Fig. 4.7.** Current density-voltage characteristics curves of DSSCs with the pre-treatment of FTO layer with acids sensitized by: (1) Hibiscus Rosa Sinensis (2) Hibiscus Sabariffa (3) Rosa Damascena (4) Hibiscus Rosa Sinensis (5) Hibiscus Sabariffa (6) Rosa Damascena. The upper panels were presented in acids for 5 minutes whereas the lower panels for 10 minutes.

Table 4.2 and Table 4.3 shows the photovoltaic parameters of the pre-treated DSSCs using the hydrochloric (HCl), phosphoric ( $\text{H}_3\text{PO}_4$ ), and nitric ( $\text{HNO}_3$ ) acids for 5 then 10 minutes, respectively.

**Table 4.2** Photovoltaic parameters of the DSSCs using the treated FTO with the acids for 5 minutes.

Dye	Acids	$V_{oc}$ (V)	$J_{sc}$ (mA/cm <sup>2</sup> )	$V_m$ (V)	$J_m$ (mA/cm <sup>2</sup> )	FF	H %
Hibiscus Rosa Sinensis	Untreated	0.55	0.23	0.41	0.15	0.49	0.06
	H <sub>3</sub> PO <sub>4</sub>	0.56	0.20	0.45	0.15	0.60	0.07
	HCl	0.54	0.26	0.41	0.18	0.53	0.07
	HNO <sub>3</sub>	0.56	0.28	0.45	0.19	0.55	0.09
Hibiscus Sabdariffa	Untreated	0.46	1.18	0.32	0.89	0.51	0.28
	H <sub>3</sub> PO <sub>4</sub>	0.46	1.20	0.34	0.87	0.54	0.30
	HCl	0.47	1.19	0.35	0.92	0.57	0.32
	HNO <sub>3</sub>	0.46	1.13	0.32	0.78	0.48	0.25
Rosa Damascena	Untreated	0.53	0.35	0.41	0.26	0.56	0.11
	H <sub>3</sub> PO <sub>4</sub>	0.51	0.28	0.40	0.19	0.52	0.08
	HCl	0.51	0.29	0.40	0.20	0.54	0.08
	HNO <sub>3</sub>	0.53	0.28	0.42	0.19	0.54	0.08

The J-V characteristics of DSSCs of the treated FTO with acids for 5 minutes under an illumination of 100 mW/cm<sup>2</sup> are shown in the upper panels of Fig. 4.7. Table 4.2 presents the Photovoltaic parameters of the same DSSCs sensitized by the three natural dyes under the previous conditions. The  $V_{oc}$  ranges between 0.46 V for DSSCs sensitized with Hibiscus Sabdariffa extract when treating FTO with H<sub>3</sub>PO<sub>4</sub> and HNO<sub>3</sub> acids for 5 minutes and 0.56 V for the cells dyed with Hibiscus Rosa Sinensis when treating FTO with H<sub>3</sub>PO<sub>4</sub> and HNO<sub>3</sub> acids for 5 minutes. The  $J_{sc}$  has a maximum value of 1.20 mA/cm<sup>2</sup> for the DSSC sensitized with the dye extracted from Hibiscus Sabdariffa when treating FTO with H<sub>3</sub>PO<sub>4</sub> acid for 5 minutes, and a minimum value of 0.2 mA/cm<sup>2</sup> for the DSSC sensitized with the dye extracted from Hibiscus Rosa Sinensis when treating FTO with H<sub>3</sub>PO<sub>4</sub> acid for 5 minutes.

The fill factor of the fabricated cells changes from 48% to 60%. The highest fill factor was obtained for the DSSC sensitized with the extract of Hibiscus Rosa Sinensis when treating FTO with H<sub>3</sub>PO<sub>4</sub> acid for 5 minutes and the lowest fill factor was observed for the cell dyed with Hibiscus Sabdariffa when treating FTO with HNO<sub>3</sub> acid for 5 minutes. The highest efficiency has a value of 0.32% for the DSSC sensitized with Hibiscus Sabdariffa when treating FTO with HCl acid for 5 minutes, while the lowest efficiency has the value of 0.06% for the DSSC sensitized with

Hibiscus Rosa Sinensis without treatment. The treatment of FTO layer by the three acids for 5 minutes didn't improve the efficiency when the Rosa Damascena and Hibiscus Sabdariffa dye solutions were used as photosensitizers. The pre-treatment of the FTO with  $H_3PO_4$  and HCl for 5 minutes showed an improved efficiency of 116.7% and 150% with  $HNO_3$  for the DSSC sensitized with the dye extracted from Hibiscus Rosa Sinensis.

**Table 4.3** Photovoltaic parameters of the DSSCs sensitized by natural dyes using pre-treatment the FTO by acids for 10 minutes.

Dye	Acids	$V_{oc}$ (V)	$J_{sc}$ (mA/cm <sup>2</sup> )	$V_m$ (V)	$J_m$ (mA/cm <sup>2</sup> )	FF	$\eta$ %
Hibiscus Rosa Sinensis	Untreated	0.55	0.23	0.41	0.15	0.49	0.06
	$H_3PO_4$	0.53	0.31	0.42	0.21	0.53	0.09
	HCl	0.53	0.32	0.43	0.23	0.58	0.1
	$HNO_3$	0.53	0.29	0.42	0.20	0.55	0.08
Hibiscus Sabdariffa	Untreated	0.46	1.18	0.32	0.89	0.51	0.28
	$H_3PO_4$	0.46	0.87	0.34	0.65	0.55	0.22
	HCl	0.45	1.07	0.33	0.82	0.56	0.27
	$HNO_3$	0.45	0.88	0.33	0.61	0.51	0.20
Rosa Damascena	Untreated	0.53	0.35	0.41	0.26	0.56	0.11
	$H_3PO_4$	0.51	0.23	0.38	0.14	0.45	0.05
	HCl	0.51	0.34	0.38	0.22	0.48	0.08
	$HNO_3$	0.51	0.36	0.40	0.25	0.54	0.10

The treatment of the FTO layer with acids was repeated for 10 minutes and the J-V characteristics of DSSCs are shown in the lower panels of Fig. 4.7. Table 4.3 presents the Photovoltaic parameters of the DSSCs sensitized by the three natural dyes. The  $V_{oc}$  ranges between 0.45 V for DSSCs sensitized with Hibiscus Sabdariffa extract when treating FTO with HCl and  $HNO_3$  acids for 10 minutes and 0.55 V for the cell dyed with Hibiscus Rosa Sinensis without treating. The  $J_{sc}$  has a maximum value of 1.18 mA/cm<sup>2</sup> for the DSSC sensitized with the dye extracted from Hibiscus Sabdariffa without treating, and a minimum value of 0.23 mA/cm<sup>2</sup> for the DSSC sensitized with the dye extracted from Hibiscus Rosa Sinensis without treating and for the DSSC sensitized with the dye extracted from Rosa Damascena when treating FTO with  $H_3PO_4$  acid for 10 minutes.

The fill factor of the fabricated cells changes from 45% to 58%. The highest fill factor was obtained for the DSSC sensitized with the extract of Hibiscus Rosa Sinensis when treating FTO with HCl acid for 10 minutes and the lowest fill factor was observed for the cell dyed with Rosa Damascena when treating FTO with H<sub>3</sub>PO<sub>4</sub> acid for 10 minutes. The highest efficiency has a value of 0.28% for the DSSC sensitized with Hibiscus Sabdariffa without treating whereas the lowest efficiency has the value of 0.05% for the DSSC sensitized with Rosa Damascena when treating FTO with H<sub>3</sub>PO<sub>4</sub> acid for 10 minutes. The treatment of FTO by the three acids for 10 minutes didn't improve the efficiency when the Rosa Damascena and Hibiscus Sabdariffa dye solutions were used as photosensitizers. The improvement of the efficiency of DSSC was appeared when treated FTO with H<sub>3</sub>PO<sub>4</sub>, HCl and HNO<sub>3</sub> acids for 10 minutes showed 150%, 166.7% and 133.3% improves using Hibiscus Rosa Sinensis dye solution.

The function of this treatment is to clean and events scratches on the FTO layer. This leads to decreasing of the sheet resistance of the FTO glass substrate and cause more adhesion and contact points between the TiO<sub>2</sub> film and FTO layers to improve the efficiency and reduces the fast recombination rate and the photoelectrons can be collected efficiently. Strong connection between material interfaces by these acids treatment cause higher values of fill factor [47,48] as shown in Table 4.2 and Table 4.3.

#### **4.3. Acidic treatment of TiO<sub>2</sub>**

In this process, the TiO<sub>2</sub> layer was post-treated with phosphoric acid (H<sub>3</sub>PO<sub>4</sub>), nitric acid (HNO<sub>3</sub>) and hydrochloric acid (HCl). The FTO layers were cleaned using an ultrasonic bath for 20 minutes twice, washed with distilled water and then dried in an oven at 60 °C for 30 min. The TiO<sub>2</sub> paste were spread on FTO glass substrate using doctor blade method then sintered at 450 °C for 30 min and cooled down to 100 °C in ambient air. The sintered TiO<sub>2</sub> layers were immersed in 0.1M of one of the acids for 5 min and then washed with distilled water then dried in an oven for 30 min at 60 °C. Finally, the TiO<sub>2</sub> layers were immersed in the dye solutions at room temperature for 24 hours.

### 4.3.1. J-V characterizations

**Table 4.4** Photovoltaic parameters of the DSSCs sensitized by natural dyes using post-treatment of TiO<sub>2</sub> film by acids for 5 minutes.

Dye	Acids	V <sub>oc</sub> (V)	J <sub>sc</sub> (mA/cm <sup>2</sup> )	V <sub>m</sub> (V)	J <sub>m</sub> (mA/cm <sup>2</sup> )	FF	η %
Hibiscus Rosa Sinensis	Untreated	0.55	0.23	0.41	0.15	0.49	0.06
	H <sub>3</sub> PO <sub>4</sub>	0.55	0.41	0.43	0.29	0.55	0.12
	HCl	0.57	0.36	0.44	0.27	0.58	0.12
	HNO <sub>3</sub>	0.54	0.50	0.42	0.38	0.59	0.16
Hibiscus Sabdariffa	Untreated	0.46	1.18	0.32	0.89	0.51	0.28
	H <sub>3</sub> PO <sub>4</sub>	0.43	0.23	0.32	0.15	0.48	0.05
	HCl	0.45	0.90	0.32	0.66	0.52	0.21
	HNO <sub>3</sub>	0.40	0.46	0.26	0.28	0.39	0.07
Rosa Damascena	Untreated	0.53	0.35	0.41	0.26	0.56	0.11
	H <sub>3</sub> PO <sub>4</sub>	0.52	0.23	0.41	0.17	0.58	0.07
	HCl	0.53	0.28	0.42	0.20	0.56	0.08
	HNO <sub>3</sub>	0.52	0.23	0.38	0.16	0.50	0.06

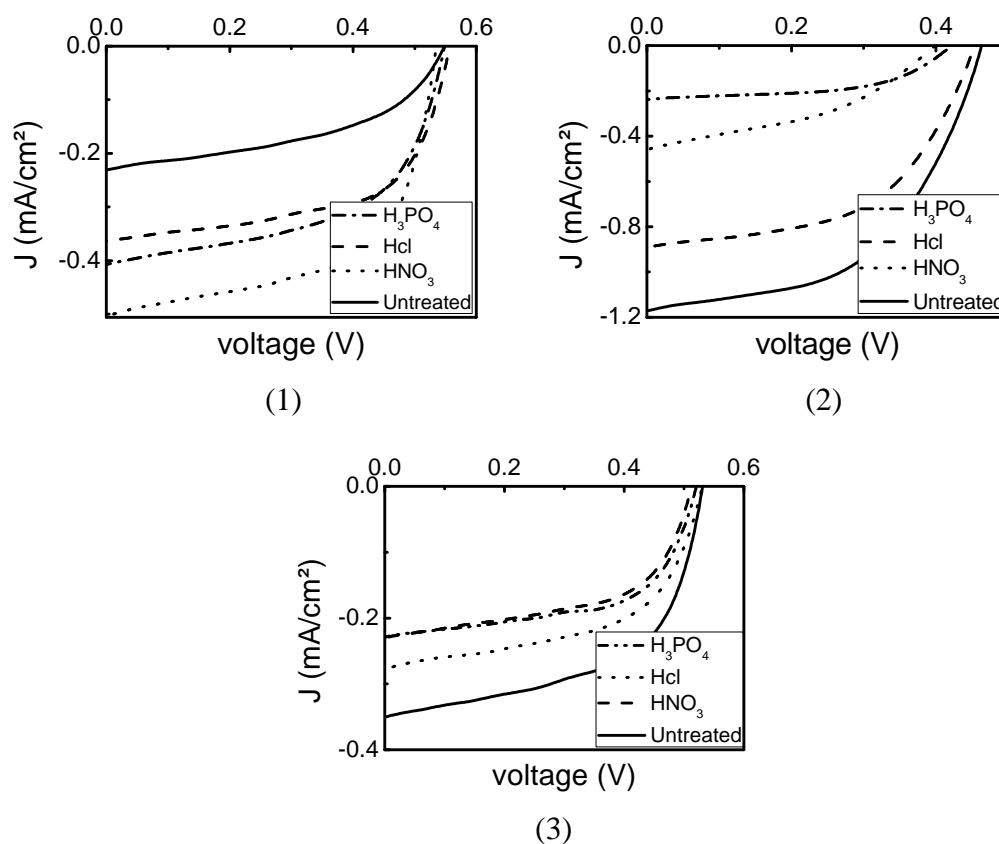


**Fig. 4.8.** Current density-voltage characteristics curves for the DSSCs sensitized by (1) Hibiscus Rosa Sinensis (2) Hibiscus Sabdariffa (3) Rosa Damascena with post-treated TiO<sub>2</sub> film by the acids for 5 minutes.

The J-V characteristics of DSSCs of the treated TiO<sub>2</sub> film with one of the three acids for 5 minutes under an illumination of 100 mW/cm<sup>2</sup> are shown in Fig. 4.8. Table 4.4 shows the photovoltaic parameters of the post-treated DSSCs using H<sub>3</sub>PO<sub>4</sub>, HCl, HNO<sub>3</sub> acids. The V<sub>oc</sub> ranges between 0.40 V for the DSSC sensitized with Hibiscus Sabdariffa extract affected by post-treatment with HNO<sub>3</sub> acid and 0.57 V for the cell dyed with Hibiscus Rosa Sinensis affected by post-treatment with HCl acid. The J<sub>sc</sub> has a maximum value of 1.18 mA/cm<sup>2</sup> for the DSSC sensitized with the dye extracted from Hibiscus Sabdariffa without treating, and a minimum value of 0.23 mA/cm<sup>2</sup> for the DSSC sensitized with the dye extracted from Hibiscus Rosa Sinensis without treating, DSSC sensitized with the dye extracted from Hibiscus Sabdariffa when treating TiO<sub>2</sub> layer with H<sub>3</sub>PO<sub>4</sub> acid and DSSCs sensitized with the dye extracted from Rosa Damascena when treating TiO<sub>2</sub> layer with H<sub>3</sub>PO<sub>4</sub> and HNO<sub>3</sub> acids.

The fill factor of the fabricated cells changes from 39% to 59%. The highest fill factor was obtained for the DSSC sensitized with the extract of Hibiscus Rosa Sinensis using treated TiO<sub>2</sub> film with HNO<sub>3</sub> acid and the lowest fill factor was observed for the cell dyed with Hibiscus Sabdariffa using treated TiO<sub>2</sub> film with HNO<sub>3</sub> acid. The highest efficiency has a value of 0.28% of the DSSC sensitized with Hibiscus Sabdariffa without treating the TiO<sub>2</sub> paste, while the lowest efficiency has the value of 0.05% of the DSSC sensitized with Hibiscus Sabdariffa when treating TiO<sub>2</sub> layer with H<sub>3</sub>PO<sub>4</sub> acid. The technique of post-treatment of TiO<sub>2</sub> by the acids for 5 minutes doesn't improve the output power and efficiency when the Rosa Damascena and Hibiscus Sabdariffa dye solutions were used as photosensitizers because the lower in the J<sub>sc</sub> and optimum current. The post-treatment of the TiO<sub>2</sub> film with H<sub>3</sub>PO<sub>4</sub> acid for 5 minutes showed an improved efficiency of 200%, 200% with HCl acid and 266.7% with HNO<sub>3</sub> acid using Hibiscus Rosa Sinensis dye solution as photosensitizer.

The reason for high short circuit density and fill factor obtained from the cell sensitized with Hibiscus Rosa Sinensis pigment may be due to the high amount of dye adsorbed onto the TiO<sub>2</sub> film against with other dyes [50]. The increase of fill factor values may be due to the strong connection between material interfaces [44].

The function of this treatment is to get TiO<sub>2</sub> film more acidic medium to faster injection of the electrons from excited state of dye into conduction band of TiO<sub>2</sub> and more free mobile electrons. The reason behind that behavior may be attributed to the improvement of TiO<sub>2</sub> film electrical conductivity by enhancing the neck points

between the nanoparticles, increasing dye loading and minimizing the recombination rate between the TiO<sub>2</sub> film and the mediator [44,51].

According to the Kubelka-Munk relationship, Fig. 4.9 shows the absorption spectra of acid treated TiO<sub>2</sub> electrode after being dyed with Hibiscus Rosa Sinensis and that of the extract from Hibiscus Rosa Sinensis in ethanol.

The absorption spectrum for the extracted dye in ethanol shows a peak at a wavelength of 548 nm. It can be observed that the absorption spectrum for that adsorbed onto acid treated TiO<sub>2</sub> film with HNO<sub>3</sub>, HCl, H<sub>3</sub>PO<sub>4</sub> acids shows a wider one at a wavelength of (581 nm, 572 nm, 553 nm) respectively. This refers to the red shifted towards higher wavelength according to the bonding strength between anthocyanin and TiO<sub>2</sub> ions [49].

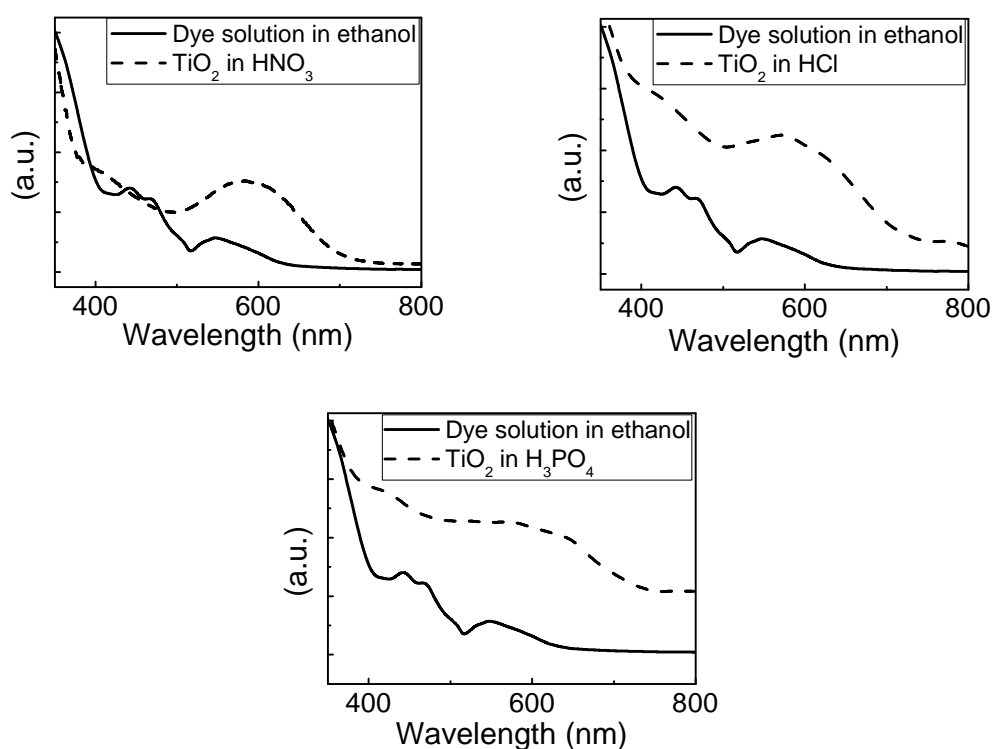


**Fig. 4.9** Absorption spectra of Hibiscus Rosa Sinensis extract in ethanol solution and anthocyanin adsorbed onto TiO<sub>2</sub> film treated with HNO<sub>3</sub>, HCl and H<sub>3</sub>PO<sub>4</sub>.

#### 4.4. Effect of the pH of dye solution

Acetic and hydrochloric acids were used to control the pH of dye solutions. Four different pH values ranging from 5.5 to 2.0 from Hibiscus Rosa Sinensis and Rosa Damascena dye solutions and those ranging from 3.0 to 1.0 from Hibiscus Sabdariffa dye solution were examined by adding 0.1 M acetic acid or 0.1 M hydrochloric acid to the dye solutions. The starting pH of the Hibiscus Rosa Sinensis, Hibiscus Sabdariffa and Rosa Damascena extracts in Ethanol were about 6.65, 3.23 and 6.15, respectively. TiO<sub>2</sub> paste was distributed on the cleaned glass substrates using doctor blade method then dyed with different pH dye solutions at room temperature for 24 hours then connected to the solar cell simulator and J-V measurements were carried out.

##### 4.4.1. J-V characterizations

The J-V characteristics of DSSC of the different pH values of the dyes under an illumination of 100 mW/cm<sup>2</sup> are shown in Fig. 4.10.

**Table 4.5** Photovoltaic parameters of the DSSCs sensitized by the dyes with changing the values of pH using acetic acid.

Dye	pH	V <sub>oc</sub> (V)	J <sub>sc</sub> (mA/cm <sup>2</sup> )	V <sub>m</sub> (V)	J <sub>m</sub> (mA/cm <sup>2</sup> )	FF	η %
Hibiscus Rosa Sinensis	Untreated	0.55	0.23	0.41	0.15	0.49	0.06
	2.0	0.31	0.05	0.14	0.02	0.19	0.003
	3.5	0.39	0.07	0.25	0.04	0.36	0.01
	4.5	0.51	0.19	0.35	0.12	0.43	0.04
	5.5	0.49	0.30	0.32	0.16	0.35	0.05
Hibiscus Sabdariffa	Untreated	0.46	1.18	0.32	0.89	0.51	0.28
	1.5	0.40	0.77	0.28	0.61	0.55	0.17
	2.0	0.42	0.84	0.28	0.60	0.47	0.17
	3.0	0.46	1.03	0.34	0.76	0.54	0.26
Rosa Damascena	Untreated	0.53	0.35	0.41	0.26	0.56	0.11
	2.0	0.46	0.24	0.34	0.16	0.49	0.05
	3.5	0.48	0.25	0.37	0.17	0.53	0.06
	4.5	0.49	0.25	0.37	0.14	0.42	0.05
	5.5	0.49	0.23	0.38	0.16	0.54	0.06

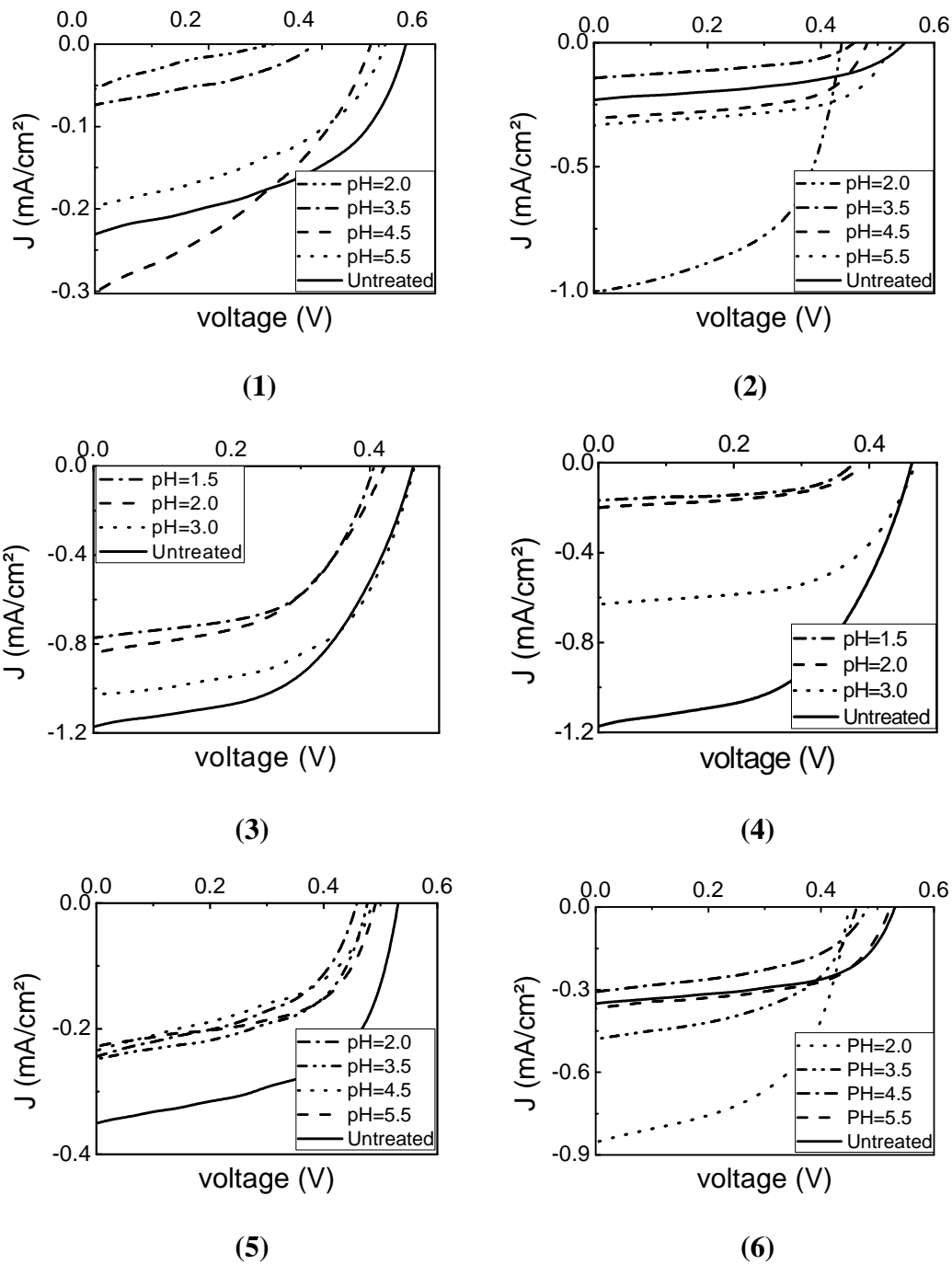


**Fig. 4.10.** Current density-voltage characteristics curves for the DSSCs sensitized by (1) Hibiscus Rosa Sinensis (3) Hibiscus Sabdariffa (5) Rosa Damascena using acetic acid to change pH of the dye, and those sensitized by (2) Hibiscus Rosa Sinensis (4) Hibiscus Sabdariffa (6) Rosa Damascena using hydrochloric acid to change pH of the dye.

Table 4.5 shows the photovoltaic parameters of the DSSCs sensitized by Hibiscus Rosa Sinensis, Hibiscus Sabdariffa and Rosa Damascena by changing the pH values using acetic acid. As shown in Table 4.5, the  $V_{oc}$  ranges between 0.31 V for DSSC sensitized with Hibiscus Rosa Sinensis of pH of 2.0 to 0.55 V for DSSC sensitized with Hibiscus Rosa Sinensis of natural pH. The  $J_{sc}$  has a maximum value of  $1.18 \text{ mA/cm}^2$  for the DSSC sensitized with the dye extracted from Hibiscus Sabdariffa of natural pH and a minimum value of  $0.05 \text{ mA/cm}^2$  for the DSSC sensitized with the dye extracted from Hibiscus Rosa Sinensis of pH of 2.0. The fill factor of the fabricated cells changes from 19% to 56%. The highest efficiency has a value of 0.28% for the DSSC sensitized with Hibiscus Sabdariffa of natural pH whereas the lowest efficiency has a value of 0.003% for the DSSC sensitized with Hibiscus Rosa Sinensis of pH of 2.0.

The acetic acid treated dyes showed poor performance in the power conversion efficiency which may be due to changing of the molecular structure of the dye and confirms that the acetic acid treatment does affect the dye molecules for minimizing absorbance and upward the conduction band of the  $\text{TiO}_2$  that decreasing the values of  $V_{oc}$  connected with low photocurrent.

Fig. 4.11 shows the DSSC efficiency as a function of the pH of the three dyes extract solutions using acetic acid. As observed from the Fig. 4.11, the efficiency is diminished with decreasing the pH for all cells except of the cell dyed with Rosa Damascena where the efficiency is enhanced from 4.5 to 3.5 pH values, after that it declines towards lowest value at pH of 2.0.

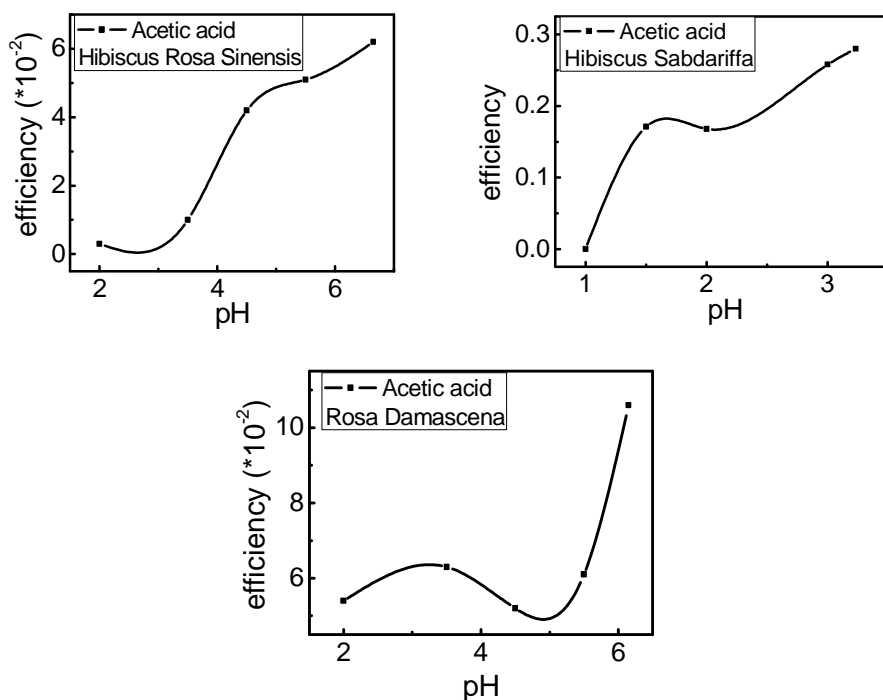


**Fig. 4.11.** DSSC efficiency versus the pH of the extract solution of three dyes using acetic acid.

The changing of pH of dyes was repeated using hydrochloric acid. The J-V characteristics of DSSC with pH was changed using HCl are shown in Fig. 4.10.

**Table 4.6** Photovoltaic parameters of the DSSCs sensitized by the dyes with changing the values pH using hydrochloric acid.

Dye	pH	$V_{oc}$ (V)	$J_{sc}$ (mA/cm <sup>2</sup> )	$V_m$ (V)	$J_m$ (mA/cm <sup>2</sup> )	FF	$\eta$ %
Hibiscus Rosa Sinensis	Untreated	0.55	0.23	0.41	0.15	0.49	0.06
	2.0	0.44	1.02	0.33	0.72	0.51	0.24
	3.5	0.46	0.14	0.35	0.09	0.42	0.03
	4.5	0.49	0.33	0.37	0.22	0.51	0.08
	5.5	0.53	0.35	0.40	0.23	0.48	0.09
Hibiscus Sabdariffa	Untreated	0.46	1.18	0.32	0.89	0.51	0.28
	1.5	0.38	0.17	0.30	0.11	0.51	0.03
	2.0	0.39	0.20	0.30	0.13	0.50	0.04
	3.0	0.47	0.63	0.35	0.49	0.58	0.17
Rosa Damascena	Untreated	0.53	0.35	0.41	0.26	0.56	0.11
	2.0	0.45	0.85	0.34	0.59	0.52	0.20
	3.5	0.46	0.48	0.36	0.31	0.50	0.11
	4.5	0.48	0.31	0.36	0.20	0.48	0.07
	5.5	0.52	0.37	0.41	0.26	0.55	0.11

Table 4.6 shows the photovoltaic parameters of the DSSCs sensitized by Hibiscus Rosa Sinensis, Hibiscus Sabdariffa and Rosa Damascena by changing the pH values using hydrochloric acid.

As shown in Table 4.6, the  $V_{oc}$  ranges between 0.38 V for DSSC sensitized with Hibiscus Sabdariffa of pH of 1.5 to 0.55 V for DSSC sensitized with Hibiscus Rosa Sinensis of natural pH. The  $J_{sc}$  has a maximum value of 1.18 mA/cm<sup>2</sup> for the DSSC sensitized with the dye extracted from Hibiscus Sabdariffa of natural pH and a minimum value of 0.14 mA/cm<sup>2</sup> for the DSSC sensitized with the dye extracted from Hibiscus Sabdariffa of pH of 2.0. The fill factor changes from 40% to 58% that affected with a low series resistance, a high shunt resistance, the connection between material interfaces and for a values of  $V_{oc}$  [44]. The highest efficiency has a value of 0.28% for the DSSC sensitized with Hibiscus Sabdariffa of natural pH, while the lowest efficiency has a value of 0.03% for the DSSC sensitized with Hibiscus Sabdariffa of pH of 1.5 and with Hibiscus Rosa Sinensis of pH of 3.5.

The changing of pH using the hydrochloric acid showed an improved efficiency of 400%, 133.3% and 150% at pH of 2.0, 4.5 and 5.5, respectively using Hibiscus Rosa Sinensis dye solution as photosensitizer and of 188% at pH of 2.0 using Rosa Damascena. The reason of the high improvement of the conversion efficiency of the DSSC sensitized with Hibiscus Rosa Sinensis dye at pH of 2.0 and pH of 5.5 and with Rosa Damascena dye at pH of 2.0 may be attributed to the strong bond between dye molecule and TiO<sub>2</sub> film and this lead to faster injection of the electrons from excited state of dye into conduction band of TiO<sub>2</sub> or to the increase of the optical absorption of the dye, as shown in Fig. 4.12. The small red shifting of the wavelength of the optical absorption peak can be considered to be due to the change of the molecular structure of the dye [44] as a result of change in pH especially at pH of 5.5 as shown in Fig. 4.12. The reason for highest short circuit density may be due to the higher amount of dye adsorbed onto the TiO<sub>2</sub> film [50]. Some factors caused high FF, the resistance for the electron transport in TCO substrate, large electrolyte thickness (distance between TiO<sub>2</sub> layer and Pt electrode), and the poor quality of Pt layer.

According to the Kubelka-Munk relationship, Fig. 4.12 shows the absorption spectra of TiO<sub>2</sub> electrode after being dyed with Hibiscus Rosa Sinensis and that of the extract from Hibiscus Rosa Sinensis in ethanol.

The absorption spectrum of the extracted dye at pH of 6.65 in ethanol shows a peak at a wavelength of 548 nm where the absorption spectrum of that at pH of 5.5 adsorbed to TiO<sub>2</sub> film shows a wider one at a wavelength of 562 nm. This refers to the red shifted towards higher wavelength according to the bonding strength between anthocyanin and TiO<sub>2</sub> ions [49], where no red shifting in the absorption spectrum of the extracted dye at pH of 2.0 adsorbed to TiO<sub>2</sub> film but show a high absorption peak of 5 times that of the extracted dye.

Fig. 4.13 shows the DSSC efficiency as a function of the pH values of the extract solutions of three dyes using hydrochloric acid. As observed from the Fig. 4.13, the efficiency when dyeing the cells of DSSCs dyed with Hibiscus Rosa Sinensis is enhanced dramatically with decreasing the pH values from 6.56 to 5.5 then it is diminished with decreasing the pH from 4.5 to 3.5 and then it is enhanced again with pH of 2.0 which corresponds the highest efficiency. For Hibiscus Sabdariffa dye, the efficiency is diminished with decreasing the pH from 3.23 to 1.0. It is diminished with decreasing the pH from 5.5 to 4.5 and then it is enhanced again with pH of 3.5 to 2.0 which corresponds the highest efficiency when using the Rosa Damascena as photosensitizer.

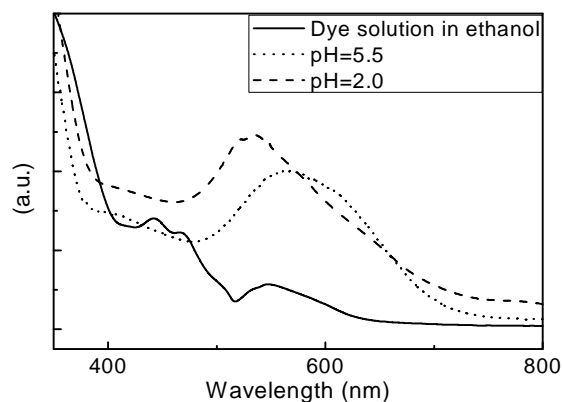


**Fig. 4.12.** Absorption spectra of Hibiscus Rosa Sinensis extract in ethanol solution and anthocyanin adsorbed onto TiO<sub>2</sub> film of pH of 2.0 and pH of 5.5.

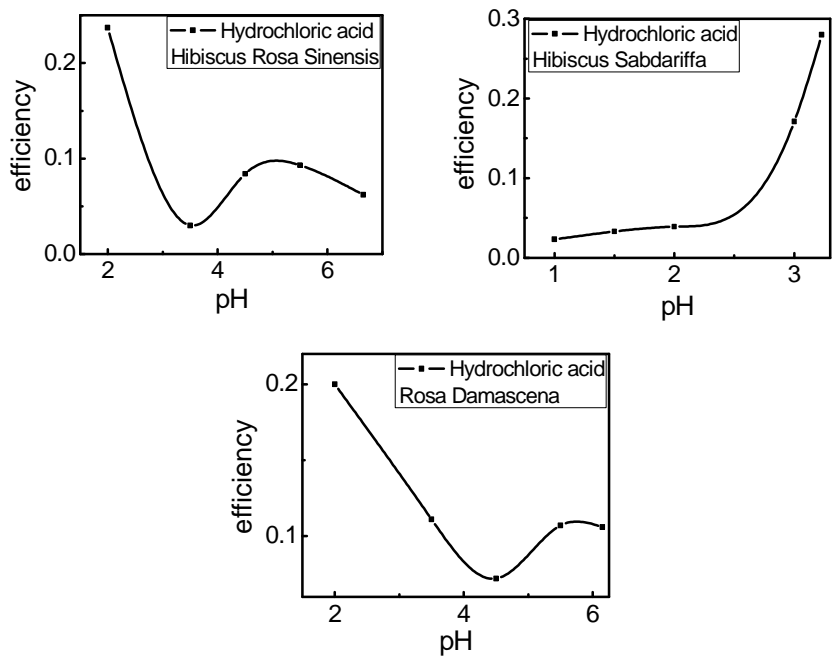


**Fig. 4.13.** DSSC efficiency versus the pH of the extract solution of three dyes using hydrochloric acid.

#### 4.5. Effect of SILAR method to improve the efficiency of DSSCs

The TiO<sub>2</sub> film was soaked in Zinc chloride (ZnCl<sub>2</sub>) solution with concentrations of 0.01, 0.05 and 0.1 M for 15 sec. after heating the film to 100 °C then immersing in boiling distilled water at temperature of 90 °C for 30 seconds then, the TiO<sub>2</sub> layers were dyed at room temperature for 24 hours. The J-V characteristics of DSSC of the treated TiO<sub>2</sub> with ZnCl<sub>2</sub> solution are shown in Fig. 4.14. This treatment was performed only for DSSCs sensitized with Hibiscus Rosa Sinensis dye.

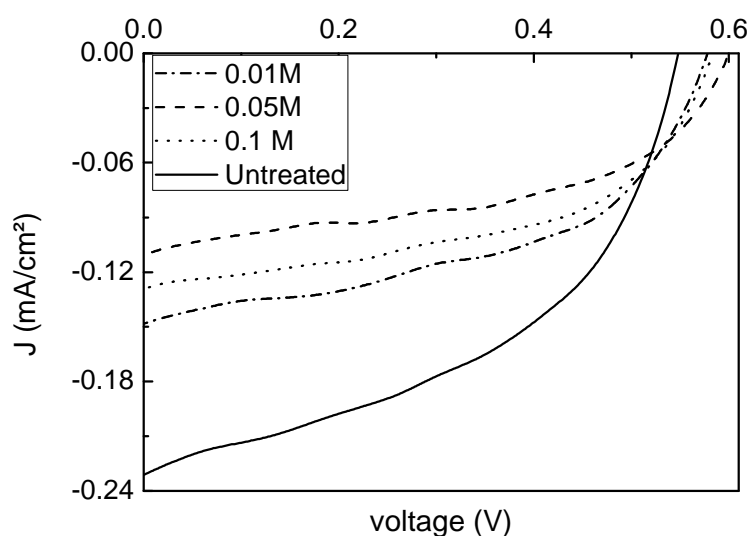


**Fig. 4.14.** Current density-voltage characteristics curves for the DSSCs sensitized by Hibiscus Rosa Sinensis using SILAR Method.

**Table 4.7** Photovoltaic parameters of the DSSCs sensitized by Hibiscus Rosa Sinensis dye using SILAR Method with three different molarities of ZnCl<sub>2</sub> solution.

Molarities	V <sub>oc</sub> (V)	J <sub>sc</sub> (mA/cm <sup>2</sup> )	V <sub>m</sub> (V)	J <sub>m</sub> (mA/cm <sup>2</sup> )	FF	η %
Untreated	0.55	0.23	0.41	0.15	0.49	0.06
0.01 M	0.58	0.15	0.45	0.09	0.47	0.04
0.05 M	0.60	0.11	0.46	0.07	0.48	0.03
0.10 M	0.58	0.13	0.45	0.08	0.48	0.04

As shown in the Table 4.7, the V<sub>oc</sub> ranges between 0.55 V for DSSC without SILAR treatment to 0.60 V for DSSC when treating the TiO<sub>2</sub> paste with 0.05 M. The J<sub>sc</sub> has a maximum value of 0.23 mA/cm<sup>2</sup> for the DSSC without SILAR treatment and a minimum value of 0.11 mA/cm<sup>2</sup> for the DSSC when treating the TiO<sub>2</sub> paste with 0.05 M. The fill factor of the fabricated cells changes from 47% to 49%. The highest

efficiency has a value of 0.06% for the DSSC without SILAR treatment, whereas the lowest efficiency has a value of 0.03% for the DSSC when treating TiO<sub>2</sub> paste with 0.05 M. The reason of the low values of the conversion efficiency of the DSSC with SILAR treatment may be attributed to the poor bonding between dye molecule and TiO<sub>2</sub> film and this leads to slow injection the electrons from excited state of the dye into the conduction band of TiO<sub>2</sub> or may be according to the poor connection between material interfaces.

#### **4.6. Electrochemical impedance spectroscopy**

Electrochemical impedance spectroscopy (EIS) was carried out for three DSSCs using Autolab PGSTAT 302N with frequency response analyzer FRA 32 Module. EIS of the DSSCs sensitized by Hibiscus Rosa Sinensis without treatment, with dye of pH of 5.5 and with post-treated TiO<sub>2</sub> layer with nitric acid for 5 minutes, were studied.

##### **4.6.1. Electrochemical impedance spectroscopy of the untreated cell**

The electrochemical impedance spectroscopy measurements were carried out in the dark and under an illumination of 100 mW/cm<sup>2</sup> at -0.4V, -0.6V, and -0.8V. Fig. 4.15 shows the Nyquist plots of the DSSC sensitized by Hibiscus Rosa Sinensis without any treatment at -0.4V, -0.6V, and -0.8V applied voltages in dark and under illumination.

As shown in Fig. 4.15 and Table 4.8, there is a decrease in the charge-transfer resistance ( $R_{CT}$ ). Electrochemical circle fit was obtained as shown in Fig. 4.16. The estimated interfacial capacitance (C) can be calculated according to the Mansfield and Hus relationship as shown in equation (4.1) from a depressed semicircle model:

$$C = Q_0 * (\omega_{max})^{(n-1)} \quad (4.1)$$

where C is estimated interfacial capacitance,  $Q_0$  is the CPE coefficient,  $\omega_{max}$  is the characteristic frequency at which the imaginary part of the impedance reaches its maximum magnitude, and n is the exponent.

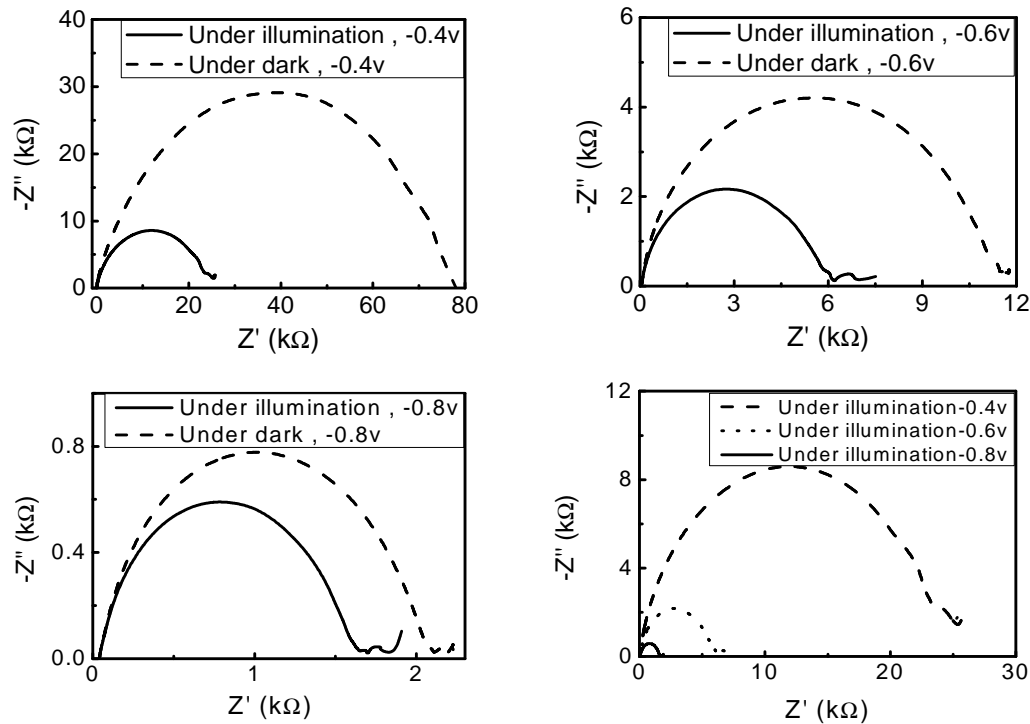


**Fig. 4.15** Nyquist plots of the DSSC sensitized by Hibiscus Rosa Sinensis without any treatment at -0.4 V, -0.6 V and -0.8 V in the dark and under an illumination of 100 mW/cm<sup>2</sup>.

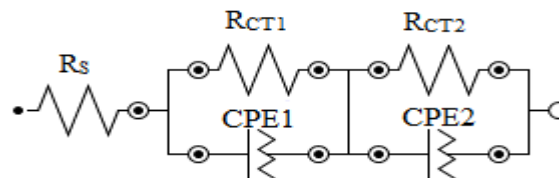


**Fig. 4.16** The equivalent circuit for the DSSC sensitized by Hibiscus Rosa Sinensis without treatments.

As shown in Fig. 4.16,  $R_s$  is the series resistance, CPE is the constant phase element, and  $R_{CT}$  is the charge-transfer resistance. Table 4.8 shows the equivalent circuit component values obtained from modeling the DSSCs sensitized by Hibiscus Rosa Sinensis without any treatment.

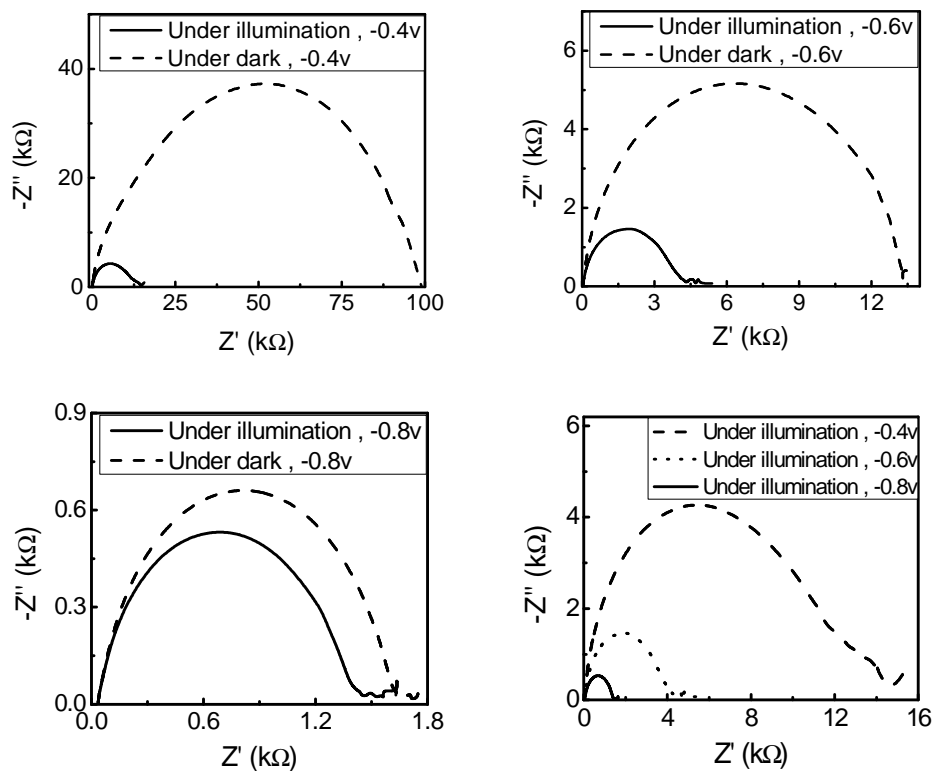
**Table 4.8** Electrochemical impedance spectroscopy results from data-fitting of Nyquist plots to the equivalent circuit model in Fig. 4.16 for the DSSC sensitized by Hibiscus Rosa Sinensis without any treatment.

Without treatments	$R_s(\Omega)$	$R_{CT1}(k\Omega)$	$C_1(\mu F)$	$R_{CT2}(k\Omega)$	$C_2(\mu F)$
-0.4v dark	40.6	74.30	1.56	-	-
-0.4v illumination	40.1	3.47	2.80	21.00	2.09
-0.6v dark	40.4	10.10	1.36	1.28	3.35
-0.6v illumination	40.0	1.60	76.30	5.05	0.93
-0.8v dark	39.0	0.28	201.00	1.91	0.84
-0.8v illumination	38.4	1.47	0.87	0.40	0.001

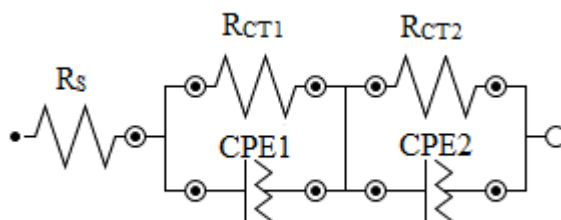
#### 4.6.2. Electrochemical impedance spectroscopy of the DSSC sensitized by Hibiscus Rosa Sinensis with post-treated $TiO_2$ layer with Nitric acid.

Fig. 4.17 shows the Nyquist plots of the DSSC sensitized by Hibiscus Rosa Sinensis with  $TiO_2$  was post treated with Nitric acid at -0.4V, -0.6V and -0.8V applied voltages.

Table 4.9 presents the equivalent circuit component values obtained from modeling the DSSCs sensitized by Hibiscus Rosa Sinensis with post treated  $TiO_2$  with Nitric acid. Electrochemical circle fit was obtained as shown in Fig. 4.18. According to Fig. 4.18 and Table 4.9, there is a decrease in the charge-transfer resistance ( $R_{CT}$ ) upon exposure to an illumination of  $100 \text{ mW/cm}^2$  at all applied voltage.



**Fig. 4.17.** Nyquist plots of the DSSC sensitized by Hibiscus Rosa Sinensis with post treated  $TiO_2$  layer with Nitric acid at  $-0.4$  V,  $-0.6$  V and  $-0.8$  V in the dark and under an illumination of  $100 \text{ mW/cm}^2$ .



**Fig. 4.18.** The equivalent circuit for the DSSC sensitized by Hibiscus Rosa Sinensis with post treated  $TiO_2$  layer with Nitric acid.

**Table 4.9** Electrochemical impedance spectroscopy results from data-fitting of Nyquist plots to the equivalent circuit model in Fig. 4.18 for the DSSC sensitized by Hibiscus Rosa Sinensis and TiO<sub>2</sub> post-treatment with Nitric acid.

TiO <sub>2</sub> post-treatment with Nitric acid	R <sub>S</sub> (Ω)	R <sub>CT1</sub> (kΩ)	C <sub>1</sub> (μF)	R <sub>CT2</sub> (Ω)	C <sub>2</sub> (μF)
-0.4v dark	33.5	92.10	1.28	-	-
-0.4v illumination	33.2	6.70	1.76	7.31	9.69
-0.6v dark	34.4	2.08	1.05	5.37	0.28
-0.6v illumination	32.9	1.44	63.30	3.34	0.78
-0.8v dark	33.1	1.23	0.94	0.40	2.09
-0.8v illumination	33	1.30	0.75	0.34	0.0007

#### 4.6.3. Electrochemical impedance spectroscopy of the DSSC sensitized by Hibiscus Rosa Sinensis solution of pH of 5.5

Fig. 4.19 shows the Nyquist plots for DSSC sensitized by Hibiscus Rosa Sinensis of pH of 5.5 in the dark and under an illumination of 100 mW/cm<sup>2</sup> at -0.4 V, -0.6 V and -0.8 V applied voltages.

Electrochemical semicircle fit were obtained at -0.4V, -0.6V, and -0.8V applied voltages and shown in Fig. 4.20. A summary of the equivalent circuit component values obtained from modeling the DSSCs sensitized by Hibiscus Rosa Sinensis of pH of 5.5 in the dark and under an illumination at chosen applied voltage can be found in Table 4.10.

According to Fig. 4.20 and Table 4.10, there is a decrease in the charge-transfer resistance (R<sub>CT</sub>) upon exposure to an illumination of 100 mW/cm<sup>2</sup> of the DSSC sensitized by Hibiscus Rosa Sinensis of pH 5.5 with hydrochloric acid at -0.4V, -0.6V and -0.8V applied voltage.

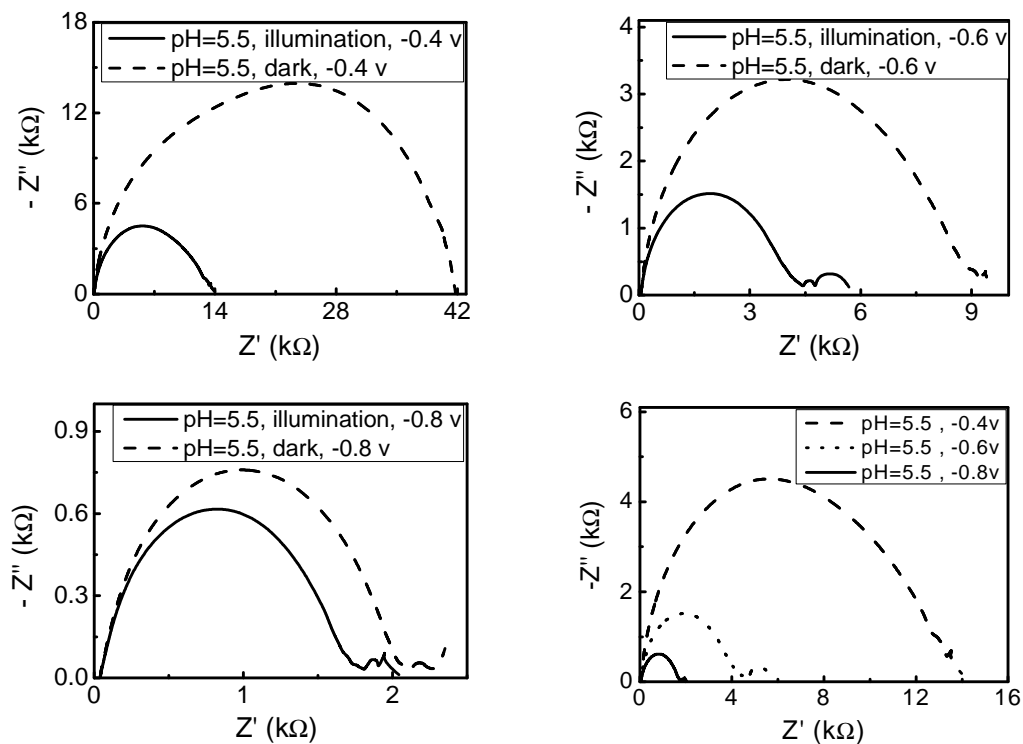


**Fig. 4.19.** Nyquist plots of the DSSC sensitized by Hibiscus Rosa Sinensis of pH of 5.5 at -0.4V in the dark and under an illumination of 100 mW/cm<sup>2</sup>.

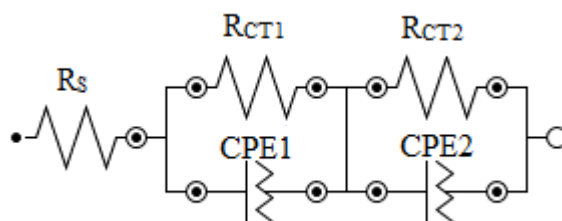


**Fig. 4.20.** The equivalent circuit for the DSSC sensitized by Hibiscus Rosa Sinensis of pH of 5.5.

**Table 4.10** Electrochemical impedance spectroscopy results from data-fitting of Nyquist plots to the equivalent circuit model in Fig. 4.20 for the DSSC sensitized by Hibiscus Rosa Sinensis of pH of 5.5.

pH 5.5 with hydrochloric acid	$R_s(\Omega)$	$R_{CT1}(k\Omega)$	$C_1(\mu F)$	$R_{CT2}(k\Omega)$	$C_2(\mu F)$
-0.4v dark	44.2	5.76	1.36	36.20	1.73
-0.4v illumination	44.6	6.66	0.87	6.81	4.62
-0.6v dark	43.7	5.85	0.66	3.35	6.89
-0.6v illumination	43.9	3.46	0.59	1.57	99.20
-0.8v dark	43.4	0.52	7.21	1.55	0.65
-0.8v illumination	43.5	0.56	226.3	0.31	0.61

Figs. 4.21, 4.22 and 4.23 represent Nyquist plots of DSSCs sensitized by Hibiscus Rosa Sinensis for the three studies mentioned above under an illumination of  $100 \text{ mW/cm}^2$  at -0.4V, -0.6V, and -0.8V applied voltages. As shown in these Figures and Tables 4.11, 4.12 and 4.13, there is a decrease in the  $R_{CT}$  for DSSCs with post treatates of  $\text{TiO}_2$  layer with nitric acid and pH of 5.5 compared with the DSSC without any treatments. The treatments lead to reduce the charge recombination at the electrolyte/ $\text{TiO}_2$ /dye interfaces and increase the electrical conductivity and the number of injected electrons from the conduction band of the dye into excited state of  $\text{TiO}_2$  film [52,53,54]. Generally, the decrease in the  $R_{CT}$  for three cells is due to the leakage current across the cell edge that caused for example from the  $\text{TiO}_2$  electrode is in direct contact with counter electrode indicates that the current has alternative ways of crossing the cell other than the desired one [55].

Giving the data in Fig. 4.24, which represents Bode plots for the DSSCs sensitized by Hibiscus Rosa Sinensis for the three studies under an illumination of  $100 \text{ mW/cm}^2$  at - applied voltages, the reduction of  $R_{CT}$  means there is a decrease in the recombination rate and indicates fast electron-transfer processes in the DSSCs [56].

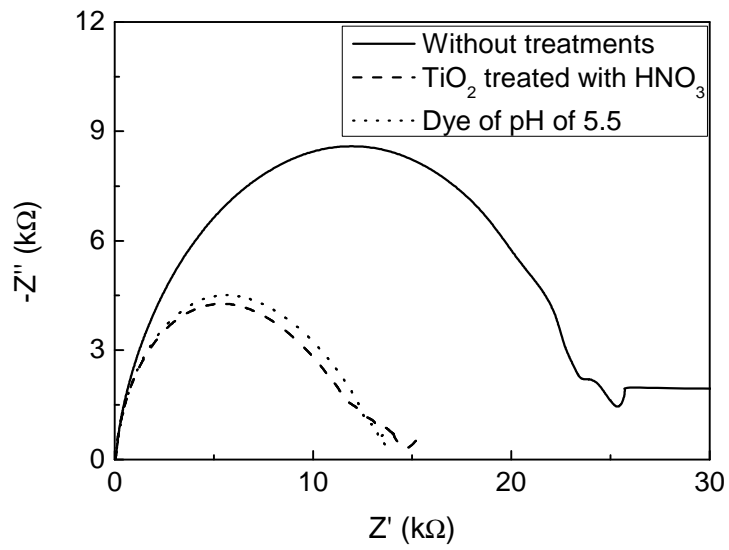


**Fig. 4.21.** Nyquist plots of DSSCs sensitized by Hibiscus Rosa Sinensis at  $-0.4V$  applied potential under an illumination of  $100 \text{ mW/cm}^2$ .

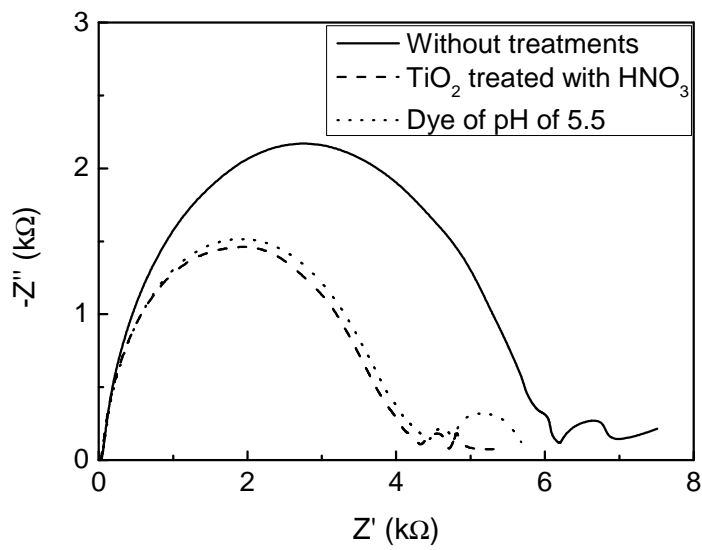


**Fig. 4.22.** Nyquist plots of DSSCs sensitized by Hibiscus Rosa Sinensis at  $-0.6V$  applied potential under an illumination of  $100 \text{ mW/cm}^2$ .

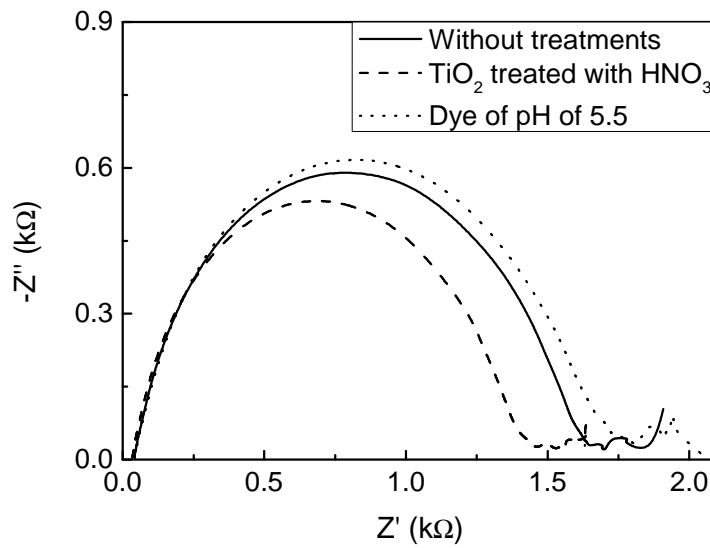


**Fig. 4.23.** Nyquist plots of DSSCs sensitized by Hibiscus Rosa Sinensis at  $-0.8\text{V}$  applied potential under an illumination of  $100\text{ mW/cm}^2$ .

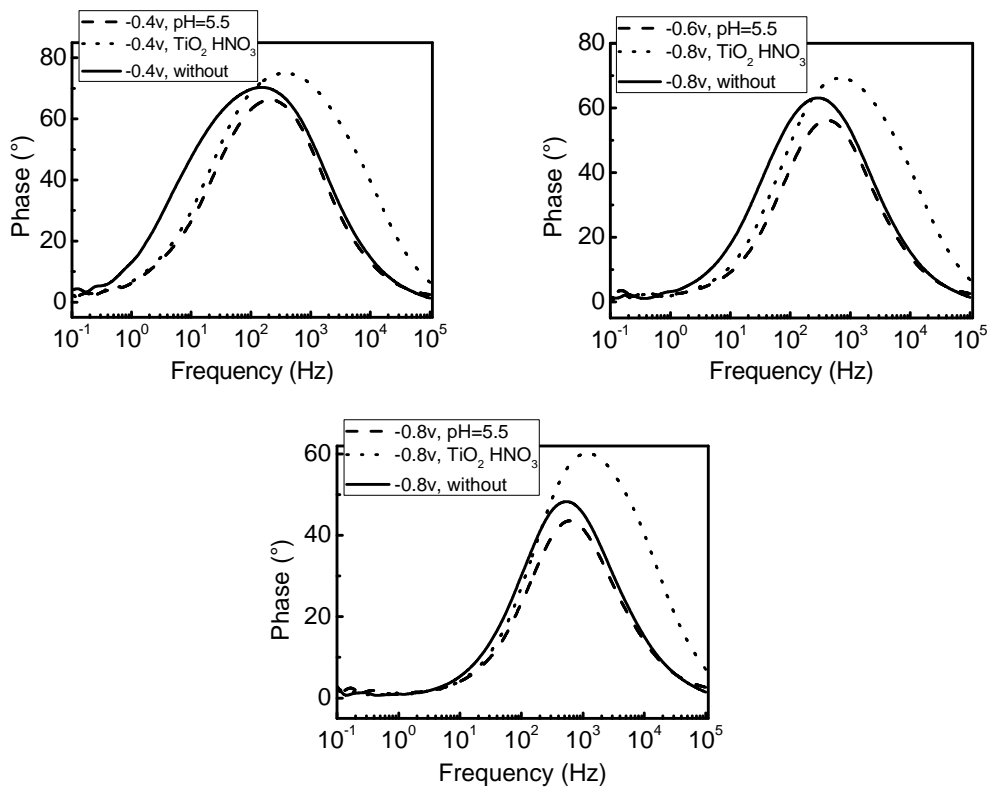


**Fig. 4.24** Bode plots of DSSCs sensitized by Hibiscus Rosa Sinensis for the three studies mentioned before under an illumination of  $100\text{ mW/cm}^2$  at  $-0.4\text{ V}$ ,  $-0.6\text{ V}$ , and  $-0.8\text{ V}$  applied voltages.

**Table 4.11** EIS results from data-fitting of Nyquist plots to the equivalent circuit model in Fig. 4.21 for the DSSCs sensitized by Hibiscus Rosa Sinensis at -0.4V applied voltage.

The treatment at -0.4V illumination	$R_s(\Omega)$	$R_{CT1} (k\Omega)$	$C_1(\mu F)$	$R_{CT2}(k\Omega)$	$C_2(\mu F)$
without treatments	40.1	3.47	2.80	21.00	2.09
nitric acid post-treatment of $TiO_2$	33.2	6.70	1.76	7.31	9.69
pH 5.5 with hydrochloric acid	44.6	6.66	0.87	6.81	4.62

**Table 4.12** EIS results from data-fitting of Nyquist plots to the equivalent circuit model in Fig. 4.22 for the DSSCs sensitized by Hibiscus Rosa Sinensis at -0.6V applied voltage.

The treatment at -0.6V illumination	$R_s(\Omega)$	$R_{CT1} (k\Omega)$	$C_1(\mu F)$	$R_{CT2}(k\Omega)$	$C_2(\mu F)$
without treatments	40.0	1.60	7.63	5.05	0.93
nitric acid post-treatment of $TiO_2$	32.9	1.44	63.30	3.34	0.78
pH 5.5 with hydrochloric acid	43.9	1.46	0.59	1.57	99.20

**Table 4.13** EIS results from data-fitting of Nyquist plots to the equivalent circuit model in Fig. 4.23 for the DSSCs sensitized by Hibiscus Rosa Sinensis at -0.8V applied voltage.

The treatment at -0.8V illumination	$R_S(\Omega)$	$R_{CT}(k\Omega)$	$C_1(\mu F)$	$R_{CT2}(k\Omega)$	$C_2(\mu F)$
without treatments	38.4	1.47	0.87	0.40	0.001
nitric acid post-treatment of $TiO_2$	33.0	1.30	0.94	0.39	2.09
pH 5.5 with hydrochloric acid	43.5	0.56	226.30	0.31	0.61

**Table 4.14** Electron lifetime calculations from Bode plots.

The treatment	f (frequency) (Hz)	$\tau_{electron}$ (ms)
-0.4V without	138.54	1.15
-0.4V nitric acid post-treatment of $TiO_2$	380.98	0.42
-0.4V pH 5.5 with hydrochloric acid	213.18	0.75
-0.6V without	298.58	0.53
-0.6V nitric acid post-treatment of $TiO_2$	692.45	0.23
-0.6V pH 5.5 with hydrochloric acid	421.28	0.38
-0.8V without	549.90	0.29
-0.8V nitric acid post-treatment of $TiO_2$	1179.77	0.13
-0.8V pH 5.5 with hydrochloric acid	617.00	0.26

Life time indication for the recombination rate. Lower recombination rate is good for high efficiency.

## Chapter Five

### Conclusions

In this thesis, the DSSCs were fabricated using  $\text{TiO}_2$  as a semiconducting layer dyed with natural dyes extracted from dried flowers. Natural dyes from three flowers were tested as sensitizers for DSSCs and they are Hibiscus Rosa Sinensis, Hibiscus Sabdariffa and Rosa Damascena. The aim of this thesis was to study the influences of several treatment process on the performance of DSSCs including the effect of changing the pH values of the dye solution using hydrochloric acid and acetic acid. Better performance was obtained with the hydrochloric acid treatment of the dye solution of Hibiscus Rosa Sinensis than the acetic acid. As observed from the results, the efficiency is enhanced dramatically with decreasing the pH values of Hibiscus Rosa Sinensis dye solution from 6.56 to 5.5 then it is diminished with decreasing the pH from 4.5 to 3.5 and then it is enhanced again with pH of 2.0 which corresponds the highest efficiency enhancement of about 400% using hydrochloric acid where the efficiency is diminished from Hibiscus Sabdariffa and Rosa Damascena dye solutions except it enhanced dramatically with decreasing the pH values from 3.5 to 2.0.

The pre-treatment of the FTO with  $\text{H}_3\text{PO}_4$  for 10 minutes showed an improved efficiency of 140%, 160% with HCl and 135% with  $\text{HNO}_3$  by using Hibiscus Rosa Sinensis dye solution. Pre-treatment leads to decreasing of the sheet resistance of the FTO glass substrate and cause more adhesion and contact points between the  $\text{TiO}_2$  film and FTO layers to improve the efficiency and reduces the fast recombination rate and the photoelectrons can be collected efficiently.

$\text{HNO}_3$ , HCl and  $\text{H}_3\text{PO}_4$  post-treated cells showed an efficiency of 0.16%, a short circuit current of  $J_{sc}$  of  $0.5 \text{ mA/cm}^2$ , an open circuit voltage of  $V_{oc}$  of 0.54 V and a fill factor (FF) of 0.59, efficiency of 0.12%, a short circuit current of  $J_{sc}$  of  $0.36 \text{ mA/cm}^2$ , an open circuit voltage of  $V_{oc}$  of 0.57 V and a fill factor of 0.58 and efficiency of 0.12%, a short circuit current of  $J_{sc}$  of  $0.41 \text{ mA/cm}^2$ , an open circuit voltage of  $V_{oc}$  of 0.55 V and a fill factor of 0.55, respectively when the Hibiscus Rosa Sinensis dye solution was used where the normal cell gave an efficiency of 0.06%, a short circuit current of  $J_{sc}$  of  $0.23 \text{ mA/cm}^2$ , an open circuit voltage of  $V_{oc}$  of 0.55 V and a fill factor of 0.49. The  $\text{HNO}_3$ , HCl and  $\text{H}_3\text{PO}_4$  treated cells showed an efficiency enhancement of about 266.7%, 200% and 200% respectively.

SILAR treatment was applied and was found to decrease the DSSC response. The reason of the low values of the conversion efficiency of the DSSC with SILAR treatment may be attributed to the poor bonding between dye molecule and  $\text{TiO}_2$  film and this leads to slow injection of the electrons from excited state of the dye into the conduction band of  $\text{TiO}_2$  or may be according to the poor connection between material interfaces.

These observations could be conferring to that the acid treatment contributed regular arrangement of the photoelectrode by the dispersion of  $\text{TiO}_2$  nanoparticles which improved the anchoring geometry of the dye on their surfaces and led to faster electron injection. The improvement of  $\text{TiO}_2$  film electrical conductivity is achieved by enhancing the neck points between the nanoparticles, minimizing the recombination rate between the interfaces and increasing dye loading.

The application of natural dye to DSSCs as a photosensitizer is promising for the realization of high cell performance, low-cost production. Incorporation of these treatments for DSSC with existing large scale manufacturing processes could open new directions for the development of low-cost solar cells in the future.

## References

- [1] G. Wolfbauer, "Electrochemistry of Dye Sensitized Solar Cells their Sensitizer and their Redox Shuttles", Monash University Clayton, (Australia), (1999).
- [2] C. J. Winter, R. L. Sizmann and L. L. Vant-Hull, "Solar Radiation Conversion", Springer- Verlag, Berlin, Heidelberg, (1991).
- [3] K. S. El-Refi, "Dye-Sensitized Solar Cells Using TiO<sub>2</sub> as a Semiconducting Layer", Master thesis, Islamic University of Gaza, Gaza, (2013).
- [4] C. Gueymard, D. Myers, and K. Emeryand, "Proposed reference irradiance spectra for solar energy systems testing", Solar Energy, Vol. 73, No. 6, pp. 443-467, (2002).
- [5] H. A. McCartney and M. H. Unsworth, "Spectral distribution of solar radiation. I: direct radiation", Quarterly Journal of the Royal Meteorological Society, Vol. 104, No. 441, PP. 699-718, (1978).
- [6] M. Zeman, "Introduction To Photovoltaic Solar Energy", Delft University of Technology, Holland, (2005).
- [7] A. Shah, P. orres, R. Tscharnner, N. Wyrsh & H. Keppner "Photovoltaic Technology: The Case for Thin-Film Solar Cells", Science, Vol. 285, No. 5427, pp. 8-692, (1999).
- [8] J. Halme, "Dye-sensitized Nanostructured and Organic Photovoltaic Cells: Technical Review and Preliminary Tests", Master Thesis, Helsinki University of Technology, (Finland), (2002).
- [9] B. O'Regan and M. Grätzel, "A low-cost, high-efficiency solar cell based on dye sensitized colloidal TiO<sub>2</sub> film", Nature, Vol. 353, No. 6346, pp. 737-740, (1991).
- [10] M. K. Nazzerruddin, A. Kay, I. Podicio, R. Humphy-Baker, E. Müller, P. Liska, N. Vlachopoulos and M. Gratzel, "Conversion of light to electricity by cis-x2bis (2,2'-bipyridyl-4,4'-dicarboxylate) ruthenium (II) charge-transfers on nanocrystalline titanium dioxide electrodes", J. Am. Chem. Soc., Vol. 115, No. 14, pp. 6382-6390, (1993).

- [11] K. Wongcharee, V. Meeyoo, S. Chavadej, "Dye-sensitized solar cell using natural dyes extracted from rosella and blue pea flowers", *Science Direct*, Vol. 91, No. 7, pp. 566-571, (2007).
- [12] Z. S. Wang, T. Yamaguchi, H. Sugihara and H. Arakawa, *Langmuir*, "Significant Efficiency Improvement of the Black Dye Sensitized Solar Cell through Protonation of TiO<sub>2</sub> Films", Vol. 21, No. 10, pp. 4272-4276, (2005) .
- [13] T. W. Lin, J. R. Lin, S. Y. Tsai, J. N. Lee, C. C. Ting, "Absorption Spectra Analysis of Natural Dyes for Applications in Dye- Sensitized Nano Solar Cells", *National Conference on Theoretical and Applied Mechanics*, Vol. 96, No. 12, pp. 21-22, (2007).
- [14] P. Luo, H. Niu, G. Zheng, X. Bai, M. Zhang, W. Wang, "From salmon pink to blue natural sensitizers for solar cells: *Canna indica* L., *Salvia splendens*, cowberry and *Solanum nigrum* L.", *Spectrochim. Acta Part A*, Vol. 74, No. 4, pp. 936-942, (2009).
- [15] H. Zhou, L. Wu, Y. Gao, T. Ma, " Dye-sensitized solar cells using 20 natural dyes as sensitizers", *Journal of Photochemistry and Photobiology A: Chemistry*, Vol. 219, No. 2, pp. 188-194, (2011).
- [16] H. J. Kim<sup>1</sup>, D. J. Kim, S.N. Karthick, K.V. Hemalatha, C. J. Raj, S. Ok, Y. Choe, "Curcumin Dye Extracted from *Curcuma longa* L. Used as Sensitizers for Efficient Dye-Sensitized Solar Cells", *Int. J. Electrochem. Sci.*, Vol. 8, No. 6, pp. 8320-8328, (2013).
- [17] J. Burschka, N. Pellet, Soo-J. Moon, R. Humphry-Baker, P. Gao, M. Nazeeruddin, and M. Gratzel, "Sequential deposition as a route to high-performance perovskite-sensitized solar cells", *Nature*, Vol. 499, No. 7458, pp. 316-319 (2013).
- [18] S. Suhaimi, M. M. Shahimin, Z.A. Alahmed, J. Chysky, A. H. Reshak, "Materials for Enhanced Dye-sensitized Solar Cell Performance: Electrochemical Application", *Int. J. Electrochem. Sci.*, Vol. 10, No. , pp. 2859-2871, (2015).

- [19] A. Zulkifili, T. Kento, M. Daiki, and A. Fujiki, "The Basic Research on the Dye-Sensitized Solar Cells (DSSC)", *Journal of Clean Energy Technologies*, Vol. 3, No. 5, pp. 382-387, (2015).
- [20] S. A. Taya, T. M. El-Agez, H. S. El-Ghamri and M. S. Abdel-Latif, "Dye-sensitized solar cells using fresh and dried natural dyes", *International Journal of Materials Science and Applications*, Vol. 2, No. 2, pp. 37-42, (2013).
- [21] T. M. El-Agez, A. A. El Tayyan, A. Al-Kahlout, S. A. Taya and M. S. Abdel-Latif, "Dye-sensitized solar cells based on ZnO films and natural dyes", *International Journal of Materials and Chemistry*, Vol. 2, No. 3, pp. 105-110, (2012).
- [22] M. S. Abdel-Latif, T. M. El-Agez, S. A. Taya, A. Y. Batniji and H. S. El-Ghamri, "Plant Seeds-Based Dye-Sensitized Solar Cells", *Journal of Materials Sciences and Applications*, Vol. 4, No. 9, pp. 516-520, (2013).
- [23] I. M. Radwan, "Dye Sensitized Solar Cells Based on Natural Dyes Extracted from Plant Roots", Master thesis, Islamic University of Gaza, Gaza, (2015).
- [24] M. Toivola, "Dye Sensitized Solar Cells on Alternative Substrates", Master Thesis, Alto University, Finland (2010).
- [25] A. N. Zulkifili, T. Kento, M. Daiki, and A. Fujiki, "The Basic Research on the Dye-Sensitized Solar Cells (DSSC)", *Journal of Clean Energy Technologies*, Vol. 3, No. 5, pp. 382-387, (2015).
- [26] K. Kalyanasundaram, M. Grätzel, "Applications of functionalized transition metal complexes in photonic and optoelectronic devices", *Coordination Chemistry Reviews*, Vol. 177, No. 1, pp. 347-414, (1998).
- [27] A. R. Hernandez-Martínez, M. Estevez, S. Vargas, F. Quintanilla, R. Rodríguez, "Natural Pigment-Based Dye-Sensitized Solar Cells", *Journal of Applied Research and Technology*, Vol. 10, No. 1, pp. 38-47, (2012).

- [28] G. Wolfbauer, "A channel flow cell system specifically designed to test the efficiency of redox shuttles in dye sensitized solar cells", *Solar Energy Materials and Solar Cells*, Vol. 70, No. 1, pp. 85-101, (2001).
- [29] A. Stanley, "Minimizing the dark current at the dye sensitized TiO<sub>2</sub> electrode ", *Solar Energy Materials and Solar Cells*, Vol. 52, No. 2, pp. 141-154, (1998).
- [30] Y. Cao, Y. Bai, Q. Yu, et al., "Dye-sensitized solar cells with a high absorptivity ruthenium sensitizer featuring a 2-(hexylthio)thiophene conjugated bipyridine" *The Journal of Physical Chemistry C*, Vol. 113, No. 15, pp. 6290–6297, (2009).
- [31] N. Papageorgiony, W. F. Maier, M. Grätzel, "An Iodide/Triiodide Reduction Electron catalyst for Aqueous and Organic Media", *J. Electrochem. soc.*, Vol. 144, No. 3, pp. 876-884, (1997).
- [32] A. Tolvanen, "Characterization and manufacturing techniques of dye sensitized solar cell", Master of science in technology, Helsinki University of Technology, (Finland), (2003).
- [33] D. G. Lee, J. T. Hong, G. C. Xu, H. S. Kim, K. J. Lee, S. J. Park, W. Y. Kim, H. J. Kim, "A simple dye-sensitized solar cell sealing technique using a CO<sub>2</sub> laser beam excited by 60 Hz AC discharges", *Optics and Laser Technology*, Vol. 42, No. 6, pp. 934-940, (2010).
- [34] G. Smestad, "Testing of dye-sensitized TiO<sub>2</sub> solar cells I: Experimental photocurrent output and conversion efficiencies", *Solar Energy Materials & Solar Cells*, Vol. 32, No. 3, pp. 259-272, (1994).
- [35] A. Luque, S. Hegedus, " Handbook of Photovoltaic Science and Engineering", Library of Congress, USA, (2003).
- [36] [http://www.ehow.com/info\\_11386125\\_methods-silar-deposition-thin-films.html](http://www.ehow.com/info_11386125_methods-silar-deposition-thin-films.html).

[37] M. M. Beevi, M. Anusuya, V. Saravanan, "Characterization of CdO Thin Films Prepared By SILAR Deposition Technique", International Journal of Chemical Engineering and Applications, Vol. 1, No. 2, pp. 151-154, (2010).

[38] E. Barsoukov, J. Macdonald, "Impedance Spectroscopy Theory, Experiment, and Applications", Library of Congress, USA, (2005).

[39] <https://www.uantwerpen.be/en/rg/axes/service/equipment/electrochemistry/metrohm-autolab-pgst>.

[40] M. Kendig, J. Scully, "Basic Aspects of Electrochemical Impedance Application for the Life Prediction of Organic Coatings on Metals", The Journal of Science and Engineering, Vol. 46, No. 1, pp. 22-29, (1990).

[41] <http://www.thermoscientific.com/en/product/genesys-10s-uv-vis/spectrophotometer.html>.

[42] T. Ma, W. M. Johnson, A. Koran, "The Color Accuracy of the Kubelka-Munk Theory for Various Colorants in Maxillofacial Prosthetic Material", J Dent Res, Vol. 66, No. 9, pp. 1438-1444, (1987).

[43] [www.thermoscientific.com/uv-vis](http://www.thermoscientific.com/uv-vis).

[44] J. M. R. C. Fernando and G. K. R. Senadeera, "Natural anthocyanins as photosensitizers for dye-sensitized solar devices" Current Science, Vol. 95, No. 5, pp. 663-666, (2008).

[45] R. F. Mansa, G. Govindasamy, Y. Y. Farm, H. Abu Bakar, J. Dayou, C. S. Sipaut, "Hibiscus Flower Extract as a Natural Dye Sensitizer for a Dye-sensitized Solar Cell", Journal of Physical Science, Vol. 25, No. 2, pp. 85-96, (2014).

[46] S. A. TAYA, T. M. EL-AGEZ, K. S. ELREFI, M. S. ABDEL-LATIF, " Dye-sensitized solar cells based on dyes extracted from dried plant leaves", Turkish Journal of Physics, Vol. 38, No. 1, pp. 1-7, (2014).

[47] M. Alhamed, A. S. Issa, A.W. Doubal, " STUDYING OF NATURAL DYES PROPERTIES AS PHOTO-SENSITIZER FOR DYE SENSITIZED SOLAR CELLS (DSSC)", Journal of Electron Devices, Vol. 16, No. 11, pp. 1370-1383, (2012).

[48] C. H. Lee, W. H. Chiu, K. M. Lee, W. F. Hsieh, J. M. Wu, " Improved performance of flexible dye-sensitized solar cells by introducing an interfacial layer on Ti substrates", Journal of Materials Chemistry , Vol. 21, No. 13, pp. 5114-5119, (2011).

[49] G. Calogero, and G. D. Marco, "Red Sicilian orange and purple eggplant fruits as natural sensitizers for dye-sensitized solar cells", Solar Energy Materials and Solar Cells, Vol. 92, No. 11, pp. 1341–1346, (2008).

[50] S. A. Taya, T. M. El-Agez, M. S. Abdel-Latif, H. S. El-Ghamri A. Y. Batniji, I. R. El-Sheikh, "Fabrication of Dye-Sensitized Solar Cells Using Dried Plant Leaves", INTERNATIONAL JOURNAL of RENEWABLE ENERGY RESEARCH, Vol. 4, No. 2, pp. 384-388, (2014).

[51] F. Cao, G. Oskam, G. J. Meyer, and P. C. Searson, "Electron transport in porous nanocrystalline TiO<sub>2</sub> photoelectrochemical cells", Journal of physical chemistry, Vol. 100, No. 42, pp. 17021-17027 (1996).

[52] S. Sarker, A. S. Ahammad, H. W. Seo, D. M. Kim, "Electrochemical Impedance Spectra of Dye-Sensitized Solar Cells: Fundamentals and Spreadsheet Calculation", International Journal of Photoenergy, Vol. 2014, No. 851705, pp. 1–17, (2014).

[53] F. Fabregat-Santiago, J. Bisquert, E. Palomares, L. Otero, D. Kuang, S. M. Zakeeruddin, and M. Gratzel, "Correlation between Photovoltaic Performance and Impedance Spectroscopy of Dye-Sensitized Solar Cells Based on Ionic Liquids", The Journal of Physical Chemistry C, Vol. 111, No. 17, pp. 6550-6560 (2007).

- [54] R. Kern, R. Sastrawan, J. Ferber, and R. Stangl, "Modeling and interpretation of electrical impedance spectra of dye solar cells operated under open-circuit conditions", *Electrochimica Acta*, Vol. 47, No. 26, pp. 4213-4225 (2002).
- [55] H. Hafez, I. Yahia, G. Sakr, M. Abdel-Mottaleb, F. Yakuphanoglu, "Extraction of the DSSC parameters based TiO<sub>2</sub> under dark and illumination conditions", *Advances in Materials and Corrosion*, Vol. 1, No. 5, pp. 8-13, (2012)
- [56] M. Zhong, J. Shi, W. Zhang, H. Han, and C. Li, "Charge recombination reduction in dye-sensitized solar cells by depositing ultrapure TiO<sub>2</sub> nanoparticles on "inert" BaTiO<sub>3</sub> films", *Materials Science and Engineering: B*, Vol. 176, No. 14, pp. 1115–1122, (2011).